NEDO-24048
77NED172
CLASS I
SEPTEMBER 1978

LICENSING TOPICAL REPORT

EVALUATION OF ACOUSTIC PRESSURE LOADS ON BWR/6 INTERNAL COMPONENTS

GENERAL ELECTRIC

NEDO-24048
77NED172
Class I
September 1978

Licensing Topical Report

EVALUATION OF ACOUSTIC PRESSURE LOADS ON BWR/6 INTERNAL COMPONENTS

Approved: D. L. Fischer
D. L. Fischer, Manager
Nuclear Engineering

Approved: E. Kiss
E. Kiss, Manager
Applied Mechanics

Approved: J. E. Wood
J. E. Wood, Manager
Nuclear Core Technology

NUCLEAR ENERGY ENGINEERING DIVISION • GENERAL ELECTRIC COMPANY
SAN JOSE, CALIFORNIA 95125

GENERAL ELECTRIC

DISCLAIMER OF RESPONSIBILITY

This document was prepared by or for the General Electric Company. Neither the General Electric Company nor any of the contributors to this document:

A. Makes any warranty or representation, express or implied, with respect to the accuracy, completeness, or usefulness of the information contained in this document, or that the use of any information disclosed in this document may not infringe privately owned rights; or

B. Assumes any responsibility for liability or damage of any kind which may result from the use of any information disclosed in this document.

TABLE OF CONTENTS

LIST OF ILLUSTRATIONS

LIST OF TABLES

ABSTRACT

Acoustic loads act on reactor vessel internals immediately after a postulated severance of a recirculation suction line at the reactor vessel nozzle. These loads result from pressure differentials across the internals, which are caused by decompression waves traveling at the speed of sound through subcooled water. The internal structures subject to acoustic loads are the shroud, shroud support and internal jet pumps.

To evaluate the design adequacy of these internal structures to these loads, the behavior of the acoustic waves must be known. General Electric uses the WHAM code to predict acoustic wave transients. The application of WHAM to BWR/6 is described and the acoustic loads are defined. Structual evaluation for these loads are briefly discussed.

It is concluded that the acoustic loads are calculated in a conservative manner for the affected vessel internals. Further, the internals are adequate to resist these loads.

1. INTRODUCTION

A sudden break in a pipe connected to a pressurized vessel causes rapid depressurization of subcooled fluid inside the vessel during the first several milliseconds after the break. A decompression wave travels from the break into the vessel, where it attenuates as it expands and is reflected from internal structures. The resulting distribution of decompression waves causes a transient pressure distribution which imposes loads on the vessel internals.

For a boiling water reactor (BWR), the worst pipe break from the point of view of acoustic loads is an instantaneous and complete severance of a recirculation suction line at the vessel nozzle. This location is in the largest line at the closest point to the vessel. These two factors maximize the acoustic loads on the internal structures. Postulated breaks in smaller lines, or at farther distances from the vessel, or with finite (non-zero) opening times result in smaller acoustic loads. For these reasons, the acoustic loads are calculated for the worst break, because these loads are the largest expected loads.

This report describes the analytical methods and models which General Electric uses to predict the magnitude and duration of acoustic loads and the associated structural responses. The basic model for the load calculation is the WHAM computer code. WHAM predicts the propagation of the acoustic wave, which originates at the location of a postulated instantaneous break at the end of the recirculation suction line vessel nozzle, and travels through subcooled water into the vessel and throughout the annular volume between the shroud and the vessel inner surface. The WHAM results are then used as inputs to other models, which predict the pressure loadings on individual structures inside the vessel.

The individual structures, or vessel internals, which are subjected to acoustic loads are the shroud, the shroud support plate and the jet pumps. These structures are shown in Figure 1-1. These are the only structures inside the

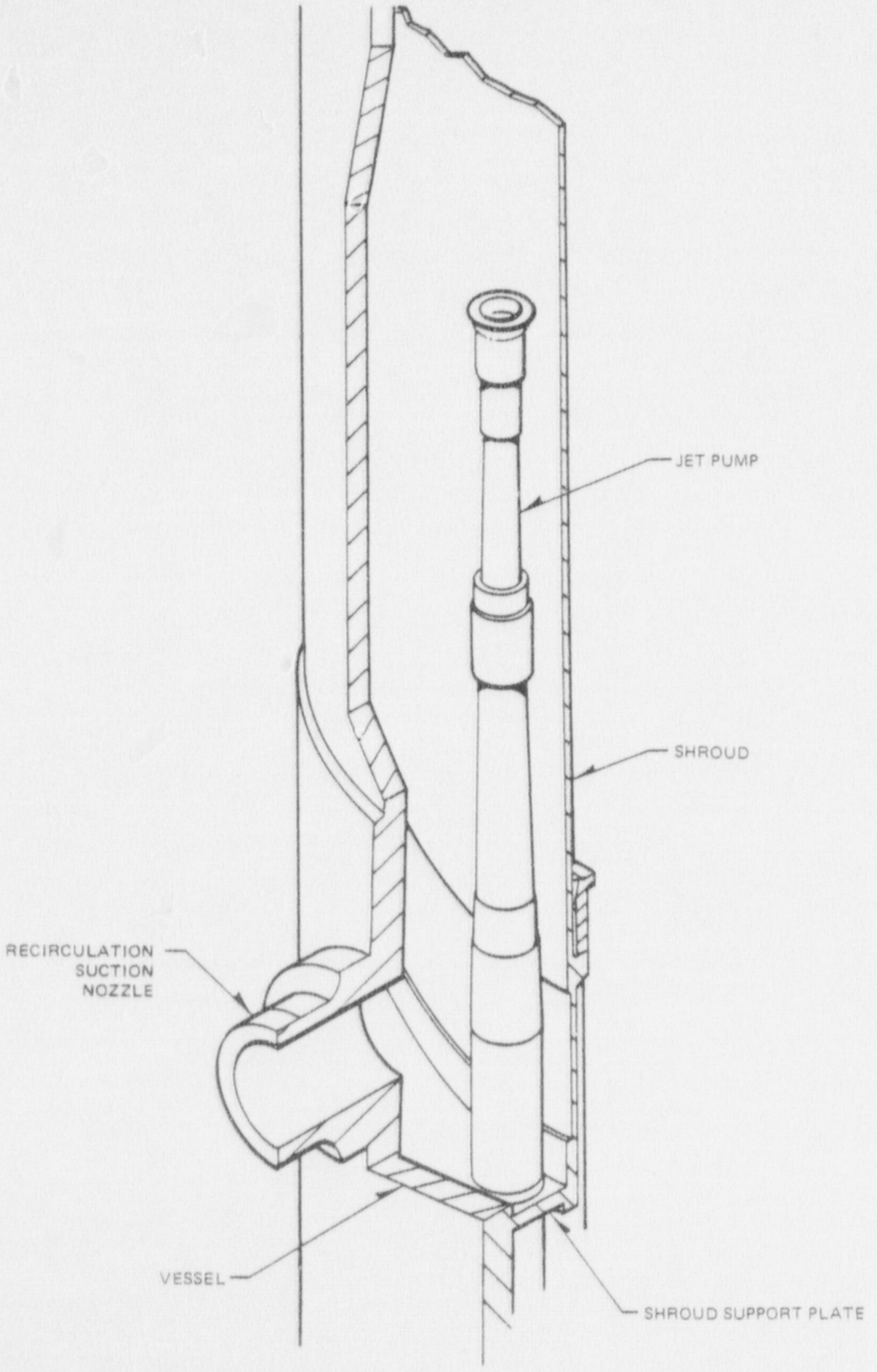

Figure 1-1. Vessel Internals Subject to Acoustic Loads

vessel surrounded by subcooled water at the start of the transient, which is the medium through which acoustic waves propagate. Acoustic waves propagate poorly (attenuate rapidly) in saturated or two-phase water. Structures in the vessel lower plenum, which also contains subcooled water, are not signif-cantly affected by acoustic waves, because of the long distance and small flow areas associated with the path from the broken recirculation line into the lower plenum. An acoustic wave which managed to travel into the vessel nozzle, up the annulus, through the jet pump throat area, down the jet pump, and into the lower plenum to impinge there on structures such as the guide tubes, would be attenuated to negligible proportions. Structures in the core and in the upper part of the annulus are surrounded by either saturated or two-phase water, and are therefore not subject to the effects of acoustic waves. Components in the unbroken recirculation loop are not affected by acoustic waves originating in the broken loop because of the distance between the two loops.

The acoustic loads are considered in the design of the internals. This report quantifies the acoustic loads and describes the evaluation of these loads on the internals.

Section 2 describes the nature of acoustic waves, experimental observations, the basis for use of the WHAM code, and the application of the WHAM code to the three vessel sizes of the BWR/6. The loads on the shroud, shroud support plate and jet pumps are described in Sections 3, 4, and 5, respectively. Section 6 summarizes the acoustic loads in a table for quick reference.

2. EVALUATION OF ACOUSTIC PRESSURE LOADS

2.1 BACKGROUND

The postulated worst pipe break in a BWR in terms of acoustic loads is an instantaneous guillotine severance of the recirculation line. Such a sudden pipe rupture will cause a relatively large amplitude decompression wave to propagate at acoustic speed from the break back into the vessel. As the wave enters the vessel, it will expand into the annular region of the downcomer around the shroud. Although the expanding wave attenuates in amplitude, it will impart some of its energy to the shroud, shroud support plate, and jet pumps.

From simple thermodynamic considerations, it would be expected that the pressure in the broken recirculation line upstream from the break would drop from an initial value of approximately 1000 psi to the vapor pressure of the fluid, approximately 800 psi for a typical water temperature of 520°F, following passage of the wave. Experimental investigations of the decompression process show that the pressure immediately behind the wave may drop momentarily below the vapor pressure. This momentary undershoot in pressure is attributed to the delay time required to cause nucleation or flashing in the fluid. During this undershoot, the fluid behaves as if it were incompressible, which results in a thermodynamic imbalance within the fluid. This imbalance causes liquid to flash to vapor, restoring thermodynamic equilibrium. The increase in vapor volume will tend to repressurize the fluid to its saturated state. The fluid dynamics of the piping and shroud may result in pressure recovery approaching the initial fluid pressure. The amplitude of the decompression wave and the magnitude of the undershoot are both important for evaluation of acoustic loads.

Additional evaluation of the decompression process has been obtained through comparative studies made with the WHAM code. The WHAM code is described in Subsection 2.4 of this report.

The experimental basis and comparative studies made with WHAM are briefly described in the Subsections 2.2 and 2.3. Subsection 2.4 gives a description of how WHAM is applied in evaluating BWR acoustic pressure loads.

2.2 EXPERIMENTAL BASIS

Insight into the decompression process has been obtained from experimental studies[1, 2, 3]. Pipes, initially filled and pressurized with subcooled water, were ruptured at one end. These pipe tests are usually referred to as shock tube experiments. Pressure measurements along the length of the pipe showed that the pressure immediately behind the decompression wave dropped to the saturated vapor pressure, and in some instances, dropped briefly below the vapor pressure. This momentary pressure undershoot during the very early part of the transient has been attributed to the nonequilibrium delay time needed to cause flashing in the fluid. The rest of the decompression process in the pipe is characterized by a considerably slower transient which is governed by the mass and energy depletion from the broken end of the pipe.

Figure 2-1 shows some typical pressure transients. The pressure drops very abruptly to near the vapor pressure following passage of the decompression wave. The remainder of the transient closely follows a saturated blowdown process.

Tests have also been conducted in conjunction with the Semi-Scale and early LOFT facilities at Idaho National Engineering Laboratory (INEL). In these tests[4], a pipe was connected to a pressure vessel which contained subcooled water as shown in Figure 2-2. The pipe was ruptured at one end. This caused a rapid decompression within the pipe near the break. The decompression within the pressure vessel occurred over a longer transient, because there was considerably more mass and energy stored in the system when compared to the simple tube studies.

General Electric Company has also conducted experiments to evaluate acoustic wave propagation. These experiments[5] were similar to those at INEL, except that the pressure vessel was initially filled with a steam-water mixture, with subcooled liquid in the lower portion of the vessel and in the pipe at

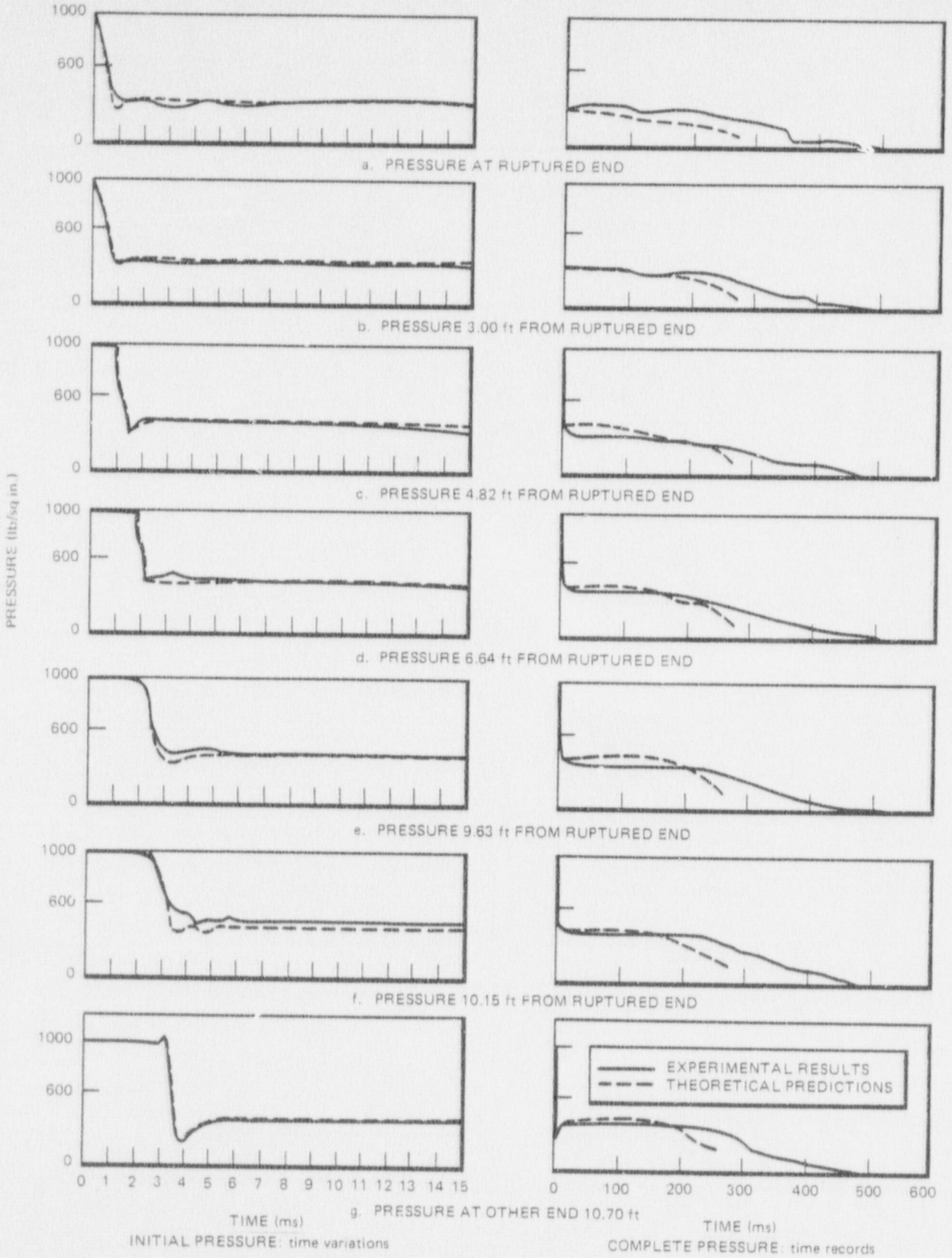

Figure 2-1. Typical Pressure Transient for blowdown from initial water conditions of 1000 psig and 467°F (saturation pressure 485 psig) (From Figure 4 of Reference 1)

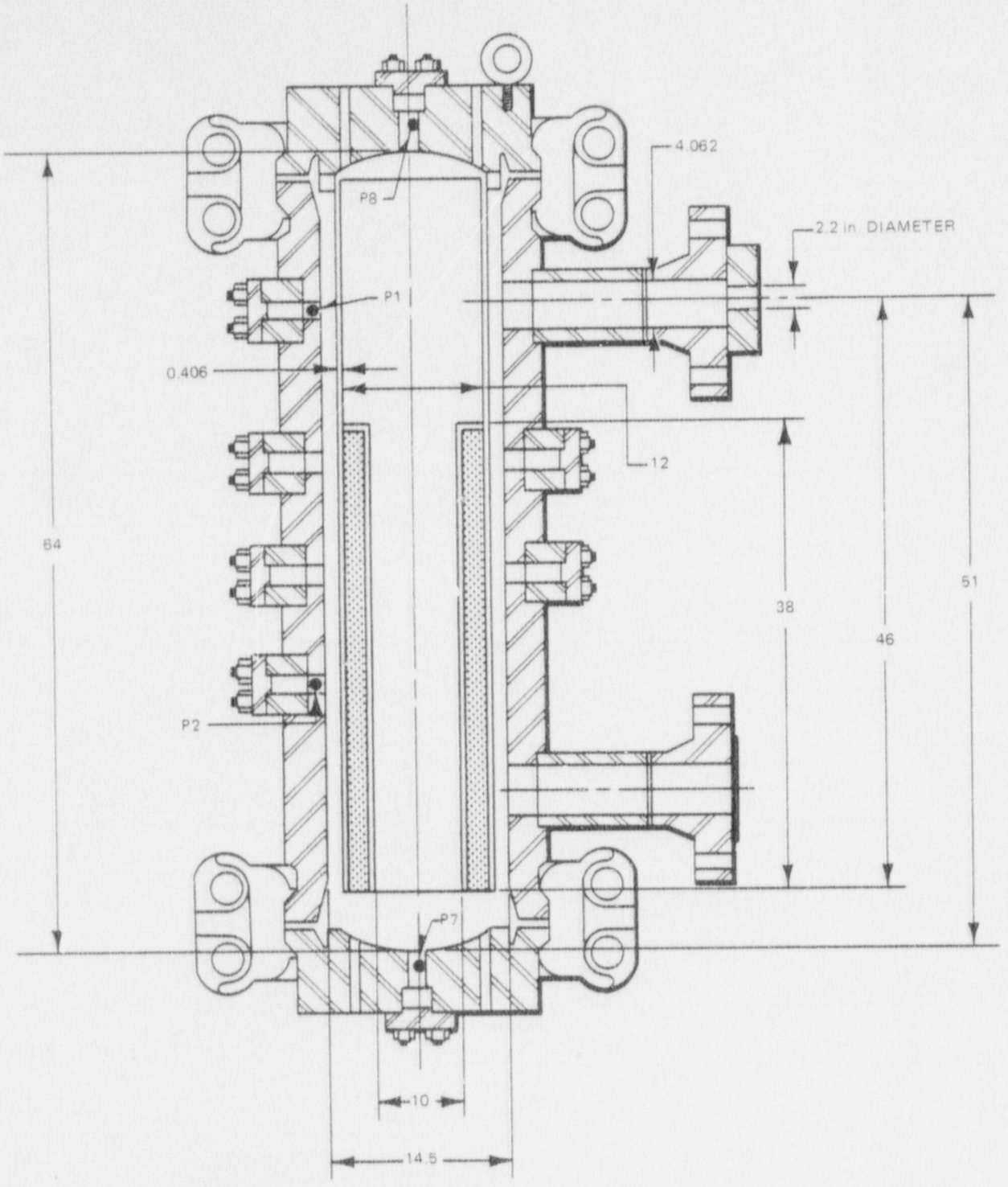

NOTE: ALL DIMENSIONS IN INCHES

Figure 2-2. Semiscale Pressurized Water Vessel Configuration for Test 711 (From Figure 2 of Reference 4)

thermodynamic conditions representative of a BWR. Figure 2-3 shows the test apparatus. The acoustic response of a steam-water BWR-type system is considerably different than for a pressurized highly subcooled water system. Figure 2-4 shows typical test results. A large amplitude decompression wave was observed in the pipe at the location of the rupture disc (break simulation) at P1 shown in Figure 2-4, but the wave amplitude entering the vessel (at P2) and within the vessel itself (at P3) was comparatively small. The compressible steam-water mixture within the vessel and the expansion of fluid within the pipe tend to dampen the magnitude of the decompression wave. A series of tests were conducted with the initial fluid subcooling as the main test parameter. Figure 2-5 summarizes the measured initial pressure undershoot (below saturation pressure) at location P2. The duration of this undershoot was typically less than 1 millisecond.

The General Electric experiments also included a shroud inside the pressure vessel[5], as shown in Figure 2-6. Measurements of pressure made in the annular region between the shroud and inside pressure vessel wall demonstrated that the wave amplitude is considerably attenuated within this region. Figure 2-7 shows typical test results for the vessel with the shroud.

2.3 PREDICTION OF DECOMPRESSION PHENOMENON

The WHAM code[6] has been used in conjunction with the INEL and GE studies discussed above to predict the observed results. In the INEL evaluation, the pressure transient at the break was not measured. It was, however, approximated from an assumption of an isentropic expansion to the saturated vapor pressure. The pressure at various points in the vessel were closely predicted by WHAM, as illustrated in Figure 2-8. The pressure transducer locations of Figure 2-8 are shown in Figure 2-2. Several test parameters were varied in the INEL studies for which WHAM calculations were made. As a result of this comparative evaluation, it was concluded that[4]:

- WHAM can accurately predict the subcooled blowdown of the LOFT apparatus (typically starting at 2300 psia and 530°F) for a break

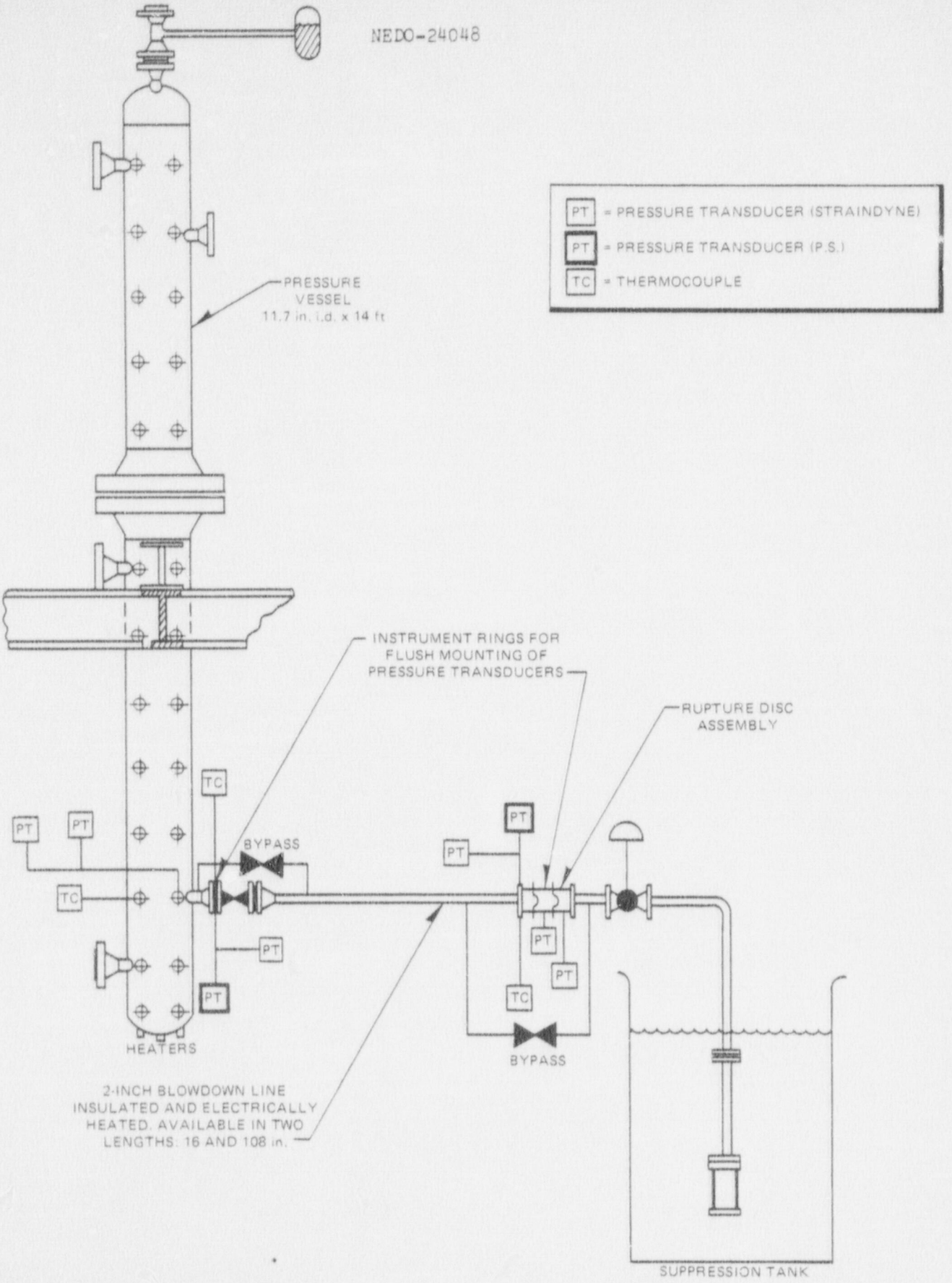

Figure 2-3. Small Blowdown Test Apparatus in One-dimensional Acoustic Wave Testing Configuration (From Figure 3-1 of Reference 5)

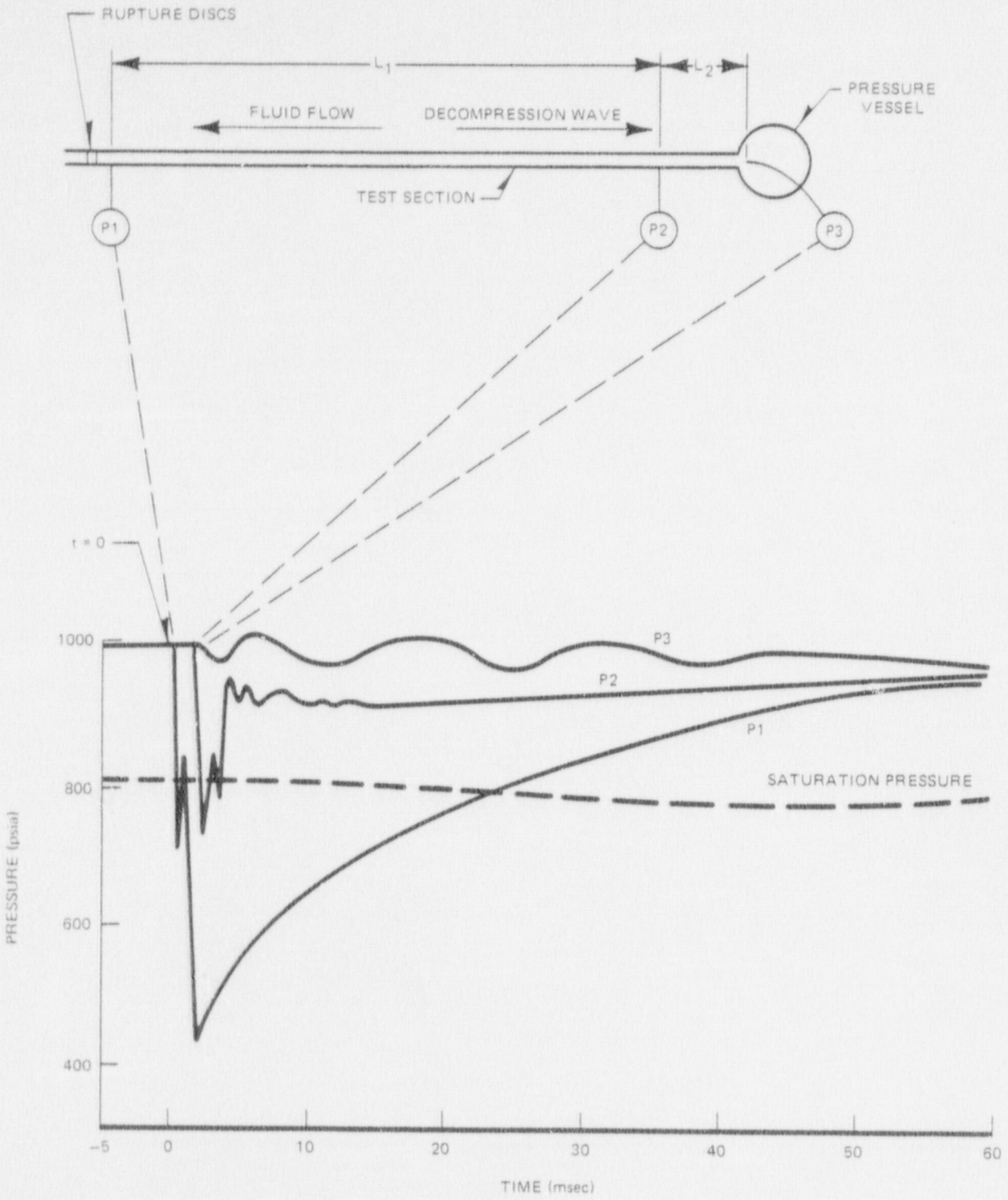

Figure 2-4. Typical Measurements from Small Blowdown Test Apparatus (From Figure 4-1 of Reference 5)

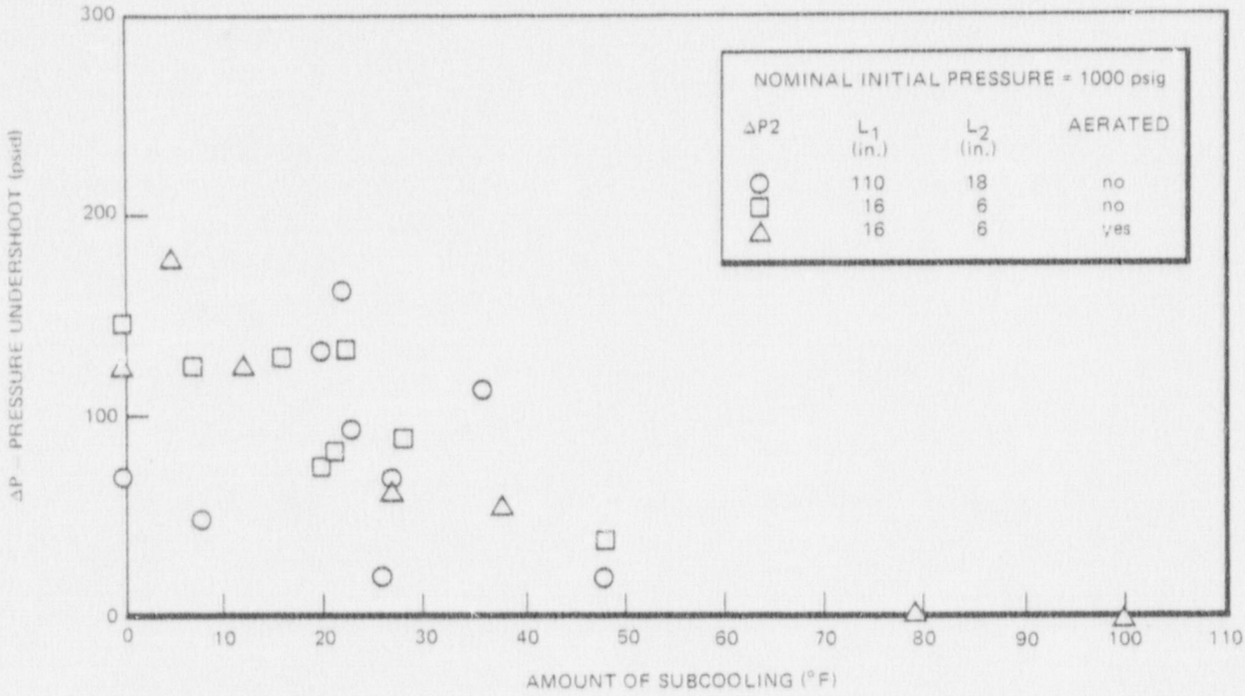

Figure 2-5. Pressure Undershoot Below Saturation Pressure from Initial Pressure of 1000 psig (From Figure 4.5 of Reference 5)

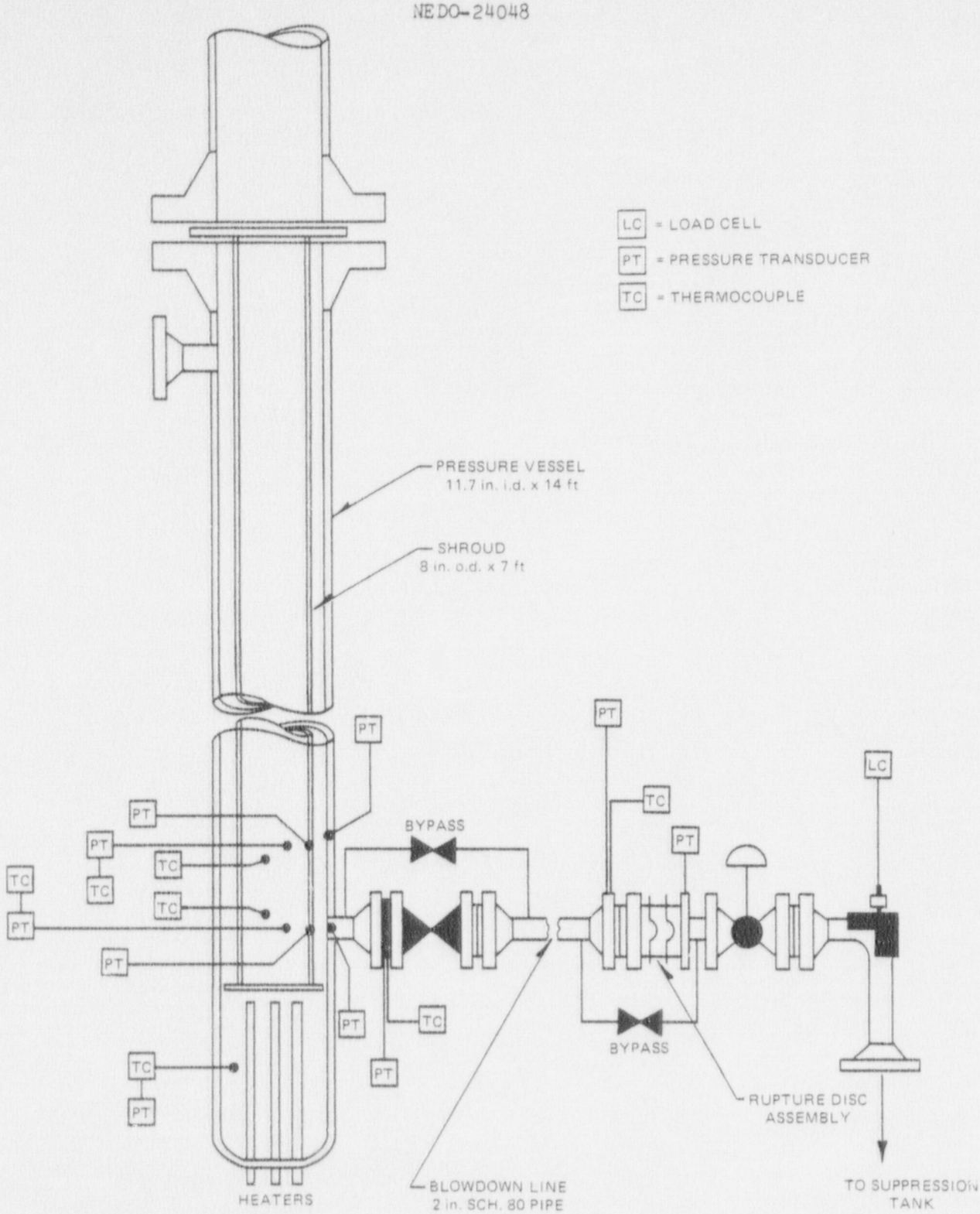

Figure 2-6. Small Blowdown Test Apparatus with Vessel Shroud in Three Dimensional Acoustic Wave Testing Configuration (From Figure 3.2 of Reference 5)

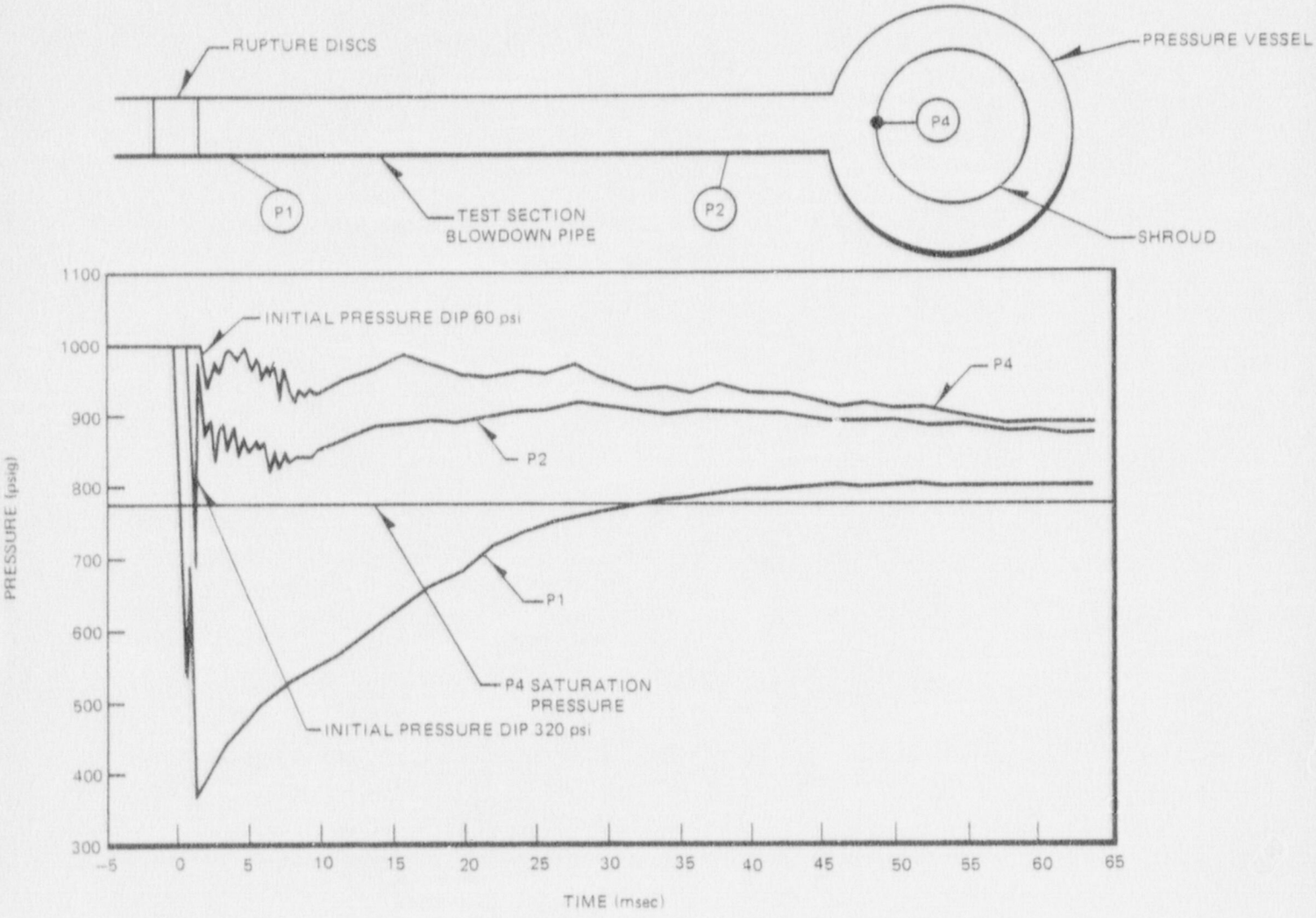

Figure 2-7. Typical Measurements from Small Blowdown Test Apparatus with Shroud (From Figure 4-2 of Reference 5)

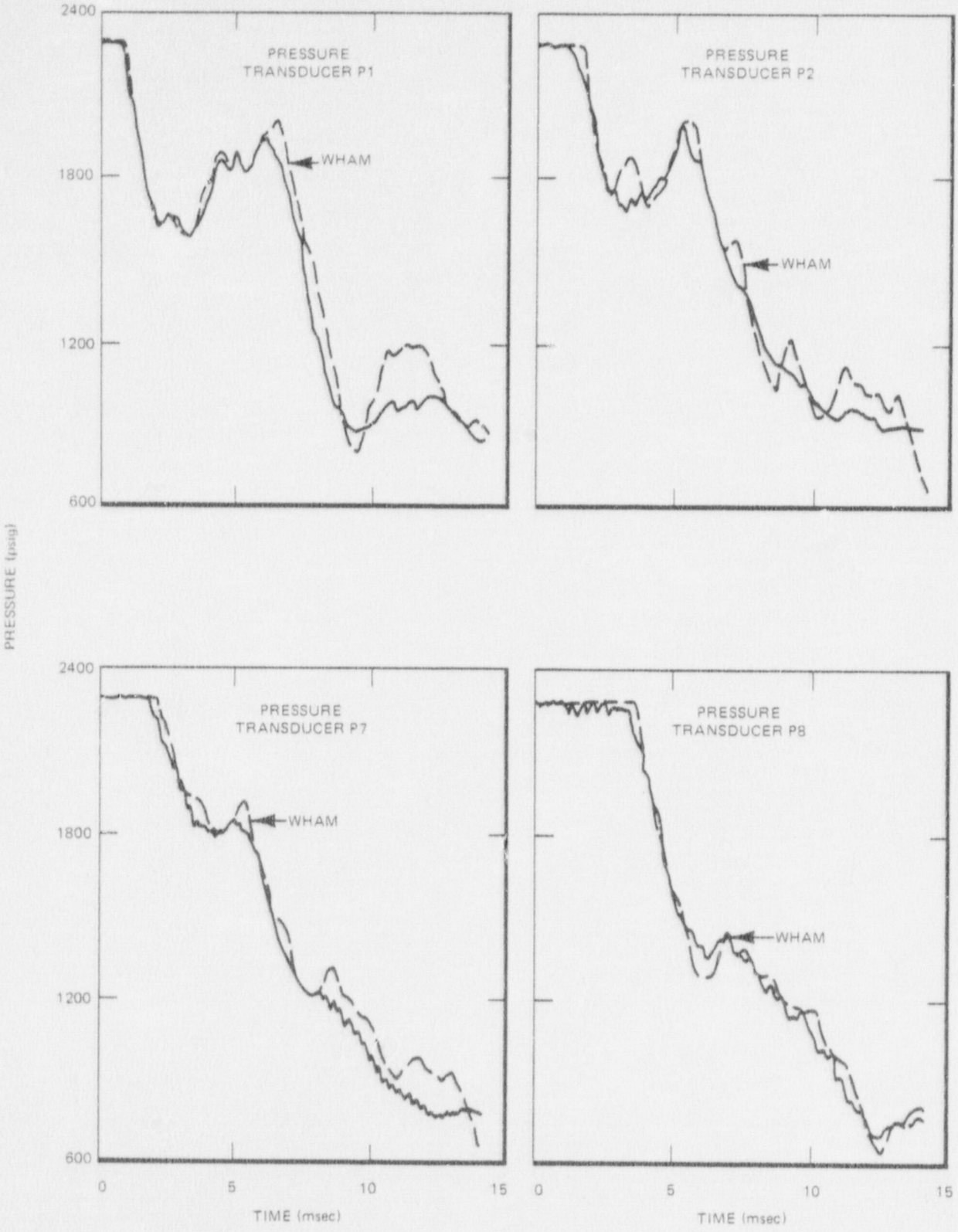

Figure 2-8. Comparison of Experimental and WHAM-Calculated Subcooled Blowdown Pressure Transients for Semiscale Test 711 (From Figure 10 of Reference 4)

area of 30% or less of the total pipe area. For this range of break areas, two-phase conditions are not observed in the broken pipe.

- For break sizes of 30% or less of the total pipe area, WHAM predictions of pressure differentials across the simulated core internals in LOFT are slightly conservative (i.e., somewhat larger than the differentials observed in the tests).

- WHAM predictions of pressure differentials for breaks in the range of 30% to 100% of the total pipe area are less accurate and more conservative when compared to test results.

- WHAM predictions for a break of 100% of the total pipe area may be unrealistically conservative.

- WHAM is an important tool for analysis of large break sizes because prediction of the initial decompression wave is accurate and is of primary importance in determining subcooled loads throughout the system.

- The capability of WHAM is such that calculated pressure histories from it are sufficiently reliable for use as forcing function input to structural dynamics codes used in the analysis of large power reactors.

WHAM has also been applied to the GE experiment whose results are shown in Figure 2-7. The equivalent piping network described in Subsection 2.4 was used in WHAM to predict the magnitude of the initial pressure dip at the shroud surface (pressure P4 in Figure 2-7). The initial pressure dip of 320 psi in pressure P2 of Figure 2-7 was applied as a boundary condition at a location in the blowdown pipe just downstream of the pressure vessel.

WHAM predicted an initial pressure dip of 150 psi at the shroud surface, compared to a measured initial pressure dip of 60 psi, as shown in Figure 2-7. It is apparent that WHAM greatly over predicts the magnitude of the initial decompression wave in the GE experiment.

The conclusions from both the INEL and GE studies regarding WHAM predictions of the initial decompression wave are the same: WHAM conservatively predicts pressure differentials across simulated core internals. Because the magnitude of the initial decompression wave determines the acoustic loading on the core internals, a conservative prediction of the initial pressure dip results in a conservative prediction of the acoustic loads.

2.4 APPLICATION OF THE WHAM CODE TO BWR EVALUATION

The basic model used by General Electric to predict acoustic pressure transients is the WHAM code. WHAM is available from the Argonne Code Center, and was originally developed by Kaiser Engineers and qualified by the Idaho Nuclear Corporation on Semiscale (LOFT) test results. Highlights of WHAM are briefly described here. The WHAM User's Manual[6] contains detailed information on WHAM.

WHAM is a one-dimensional code which predicts the transmission of acoustic waves in a piping network filled with subcooled liquid. WHAM does not describe the transmission of acoustic waves in saturated or two-phase water. In these media, local decompression causes voiding, which attenuates wave transmission. WHAM considers the fluid boundary to be rigid; there is no flexing of walls.

The WHAM user divides the piping network into a number of junctions. The junction spacing is determined by the distance traveled by the acoustic wave during one time step, which is selected with the aid of sensitivity studies. The sonic velocity may vary with junction location, depending upon local fluid conditions. Thus, the junction spacing may also vary with junction location.

WHAM can also be used to investigate the transmission of acoustic waves in two- or three-dimensional media. This is accomplished using the equivalent piping network (EPN) method, and is described in Reference 7. Basically, the fluid region under investigation is represented by a network of pipes, the volume of which is chosen to preserve the colume of the fluid region. The sonic velocity in each of the equivalent pipes is multiplied by $\sqrt{N}$, where N is the number of dimensions (two or three). The EPN technique, when used with WHAM, has been checked against selected closed form solutions.[7] Satisfactory agreement has been obtained, as long as the fluid velocity is small compared to the sonic velocity.

The EPN technique is utilized in WHAM for prediction of acoustic wave transmission in the BWR/6 geometry. Considering the qualification of WHAM with Semiscale and GE test results, the agreement of WHAM with EPN to closed-form solutions, calculated fluid velocities which are a few percent of sonic velocity, and the conservative assumptions described below, it is concluded that WHAM, coupled with the EPN technique, is an acceptable and conservative method for predicting acoustic wave transmission in the BWR/6.

For application to BWR/6, an EPN is used to model the volume between the vessel and shroud in the vicinity of the recirculation suction nozzle, as shown in Figure 2-9. Due to the relatively small curvature of the vessel and shroud, a simplified geometry consisting of a fluid region bounded by two parallel flat plates with flow out of a nozzle attached normally to one plate is considered. Table 2-1 gives the relevant dimensions of the three BWR/6 configurations analyzed with the EPN.

Symmetry of the region about the nozzle centerline allows the fluid region to be modeled by a two-dimensional EPN. The distance between the vessel and the shroud is spanned by four pipes, which was determined from sensitivity studies to be the most coarse acceptable mesh. The EPN was then extended radially outward between the plates until the limit of 100 total pipes was reached. For simplicity, vessel internals such as jet pumps are not modeled within the extent of the EPN.

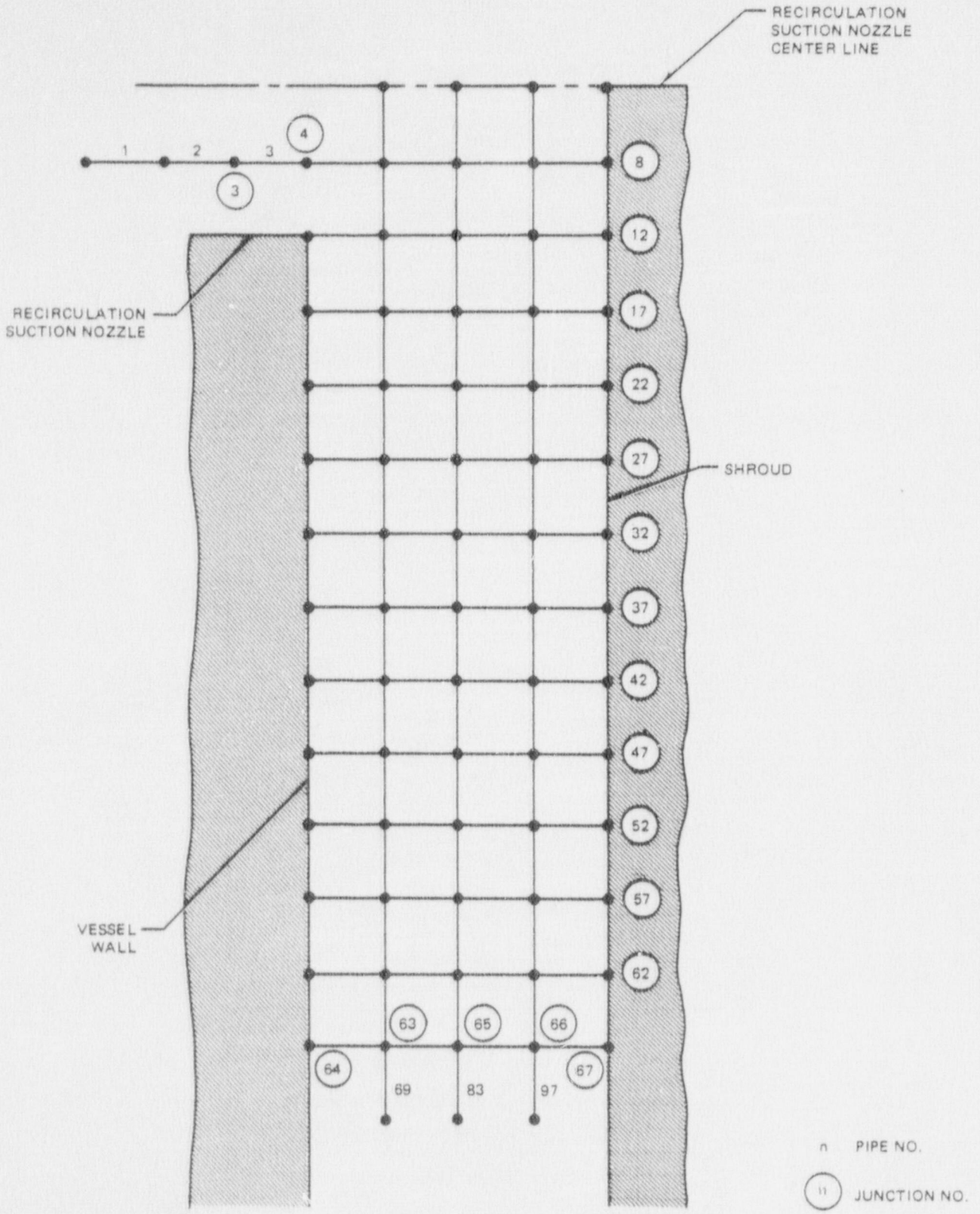

Figure 2-9. Equivalent Piping Network for BWR/6

Table 2-1

BWR/6 DIMENSIONS

Vessel i.d. (in.)	Shroud-Vessel Gap (in.)	Shroud o.d. (in.)
218	18	182
238	20	198
251	19	213

The EPN pipes (all pipes except 1, 2, and 3) are of equal length, with the exception of pipes 69, 83, and 97. To properly conserve the volume spanned by the EPN, the cross-sectional areas of the EPN pipes increase with distance from the nozzle centerline. The lengths and cross-sectional areas of pipes 69, 83, and 97 were adjusted to conserve the remaining volume of subcooled water between the vessel and the shroud.

Pipes 1, 2, and 3 on Figure 2-9 form a one-dimensional network which connects with the EPN Pipe 3 models the recirculation suction nozzle, and pipes 1 and 2 provide boundary conditions imposed by the break. The sonic speed in these three pipes corresponds to the fluid conditions initially present in the nozzle, while the sonic speed in the EPN pipes is $\sqrt{2}$ times that in the nozzle.

Three conservative assumptions were made in choosing the boundary conditions imposed by the break:

- The break area is full-sized. The break area is assumed to be the unrestricted cross-sectional flow area of the recirculation suction nozzle. This assumption is physically unrealistic and quite conservative because it ignores the presence of pipe movement limiting devices, which would prevent the broken ends of the pipe and nozzle from separating far enough to permit unimpeded break flow from the full flow area of the nozzle.

- The break opening time is instantaneous. This assumption ignores the finite opening time needed for a break to develop, which is several tens of milliseconds, due to tearing of the pipe and the inertia of the separating pipe as it accelerates from the nozzle. Sensitivity studies done by Idaho Nuclear Corporation[4] during the qualification of WHAM on Semiscale test data show that acoustic loads are eliminated when break opening times characteristic of breaking pipes (greater than 20 msec) are considered, rather than break opening times characteristic of rupturing diaphragms (less than 20 msec).

- The fluid pressure within the vessel nozzle drops quickly to and remains at a pressure which is as far below the saturation pressure as the fluid pressure was above saturation prior to the break. Before the break, the fluid in the nozzle is at 1000 psi, which is 150 psi above the saturation pressure of 850 psi. Just after the break, it is expected that the fluid pressure within the vessel nozzle will drop to saturation pressure, whereupon two-phase choking will be established at the break for the remainder of the blowdown. Experimentally, it has been observed that the pressure at the break can actually undershoot the saturation pressure momentarily, because flashing of the fluid requires a small but finite time. It is conservatively assumed that the pressure of the fluid at the end of the broken nozzle (junction (3) in Figure 2-9) falls to and remains at 700 psi during the analysis. Pipes 1 and 2 are fictitious pipes employed to cause the pressure at junction (3) to drop quickly from 1000 psi to 700 psi, and to remain constant. This assumption of a 150 psi undershoot is based on the experimental results shown in Figure 2-5.

The time interval analyzed by WHAM starts with the break, and ends when the acoustic wave reaches junctions (63) through (67) at the end of the network. This time interval covers the transmission of the initial wave through the network, and avoids the calculation of wave reflections from the end of the network (pipes 69, 83, and 97). The initial decompression wave was identified in Reference 4 as being of primary importance in determining the subcooled loads in the system.

The same EPN shown in Figure 2-9 was used for the three sizes of BWR/6 given in Table 2-1, changing only the distance between the vessel and the shroud for the three cases. The basic output from WHAM is the radial pressure distribution along the shroud surface (junctions (8), (12), (17), ... (62)) as a function of time. Typical results are shown in Figure 2-10. The times shown for each curve are measured from the time the acoustic wave passes junction (3). Note that constructive interference of reflecting waves can cause pressures in excess of the initial pressure, as shown on curve 5 of Figure 2-10. This phenomenon has been observed experimentally in the Semi-Scale tests.

The time step increment used in WHAM to calculate the results of Figure 2-10 is 0.000077 second, and the sonic velocity is 3450 ft/sec. Curve 2 of Figure 2-10 was plotted for the time when the minimum shroud pressure of 854 psi was achieved. This minimum pressure occurs on the nozzle centerline, and causes a shroud pressure differential at that point of 146 psi, because the pressure on the inside of the shroud remains at 1000 psi during the transient.

The radial acoustic pressure distributions provided by WHAM serve as input for the prediction of loads on the shroud, shroud support plate, and jet pumps. The methods used to calculate these loads are described in the following sections.

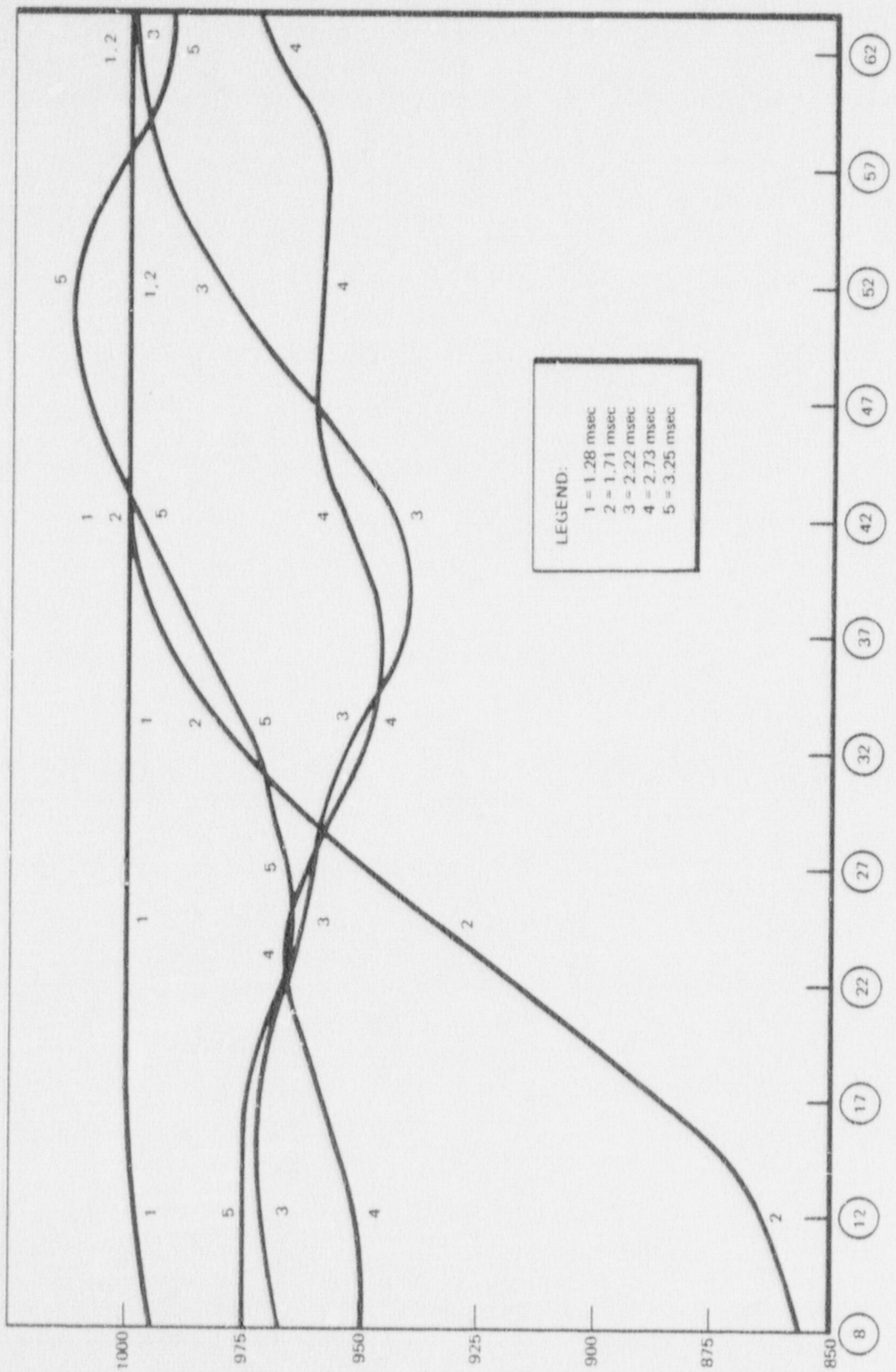

Figure 2-10. Acoustic Pressure Profiles on Shroud of BWR/6-238

3. SHROUD LOAD AND STRUCTURAL RESPONSE

3.1 SHROUD LOAD

The total load on the shroud is predicted in a separate calculation, using the radial pressure distribution from WHAM. The elements of the load calculation are shown in Figure 3-1.

Consider the area element dA in Figure 3-1. It is distance r away from the recirculation nozzle centerline, which is the z-axis. The differential pressure acting on the shroud over dA is $\Delta P(r)$

where

$$\Delta P(r) = 1000 - P(r) \text{ psi}$$

P(r) is the acoustic wave pressure predicted by WHAM at radius r, as shown in Figure 2-10, and 1000 psi is the assumed constant pressure acting on the inside shroud surface. The differential force acting outward on dA is $dF = \Delta P(r)dA$, and dA is given by $dA = rdrd\theta$, so $dF = \Delta P(r)rdrd\theta$. The net outward force on the shroud comes from dF and its mirror image dF', shown on the lower portion of Figure 3-1.

$$dF_{net} = dF \cos \phi + dF' \cos \phi$$

and because $\phi = w/R = (r \sin \theta)/R$

and $|dF'| = |dF|$

then $dF_{net} = 2dF \cos \phi$

or $$dF_{net} = 2 \Delta P(r) rdrd\theta \cos \left(\frac{r \sin \theta}{R} \right)$$

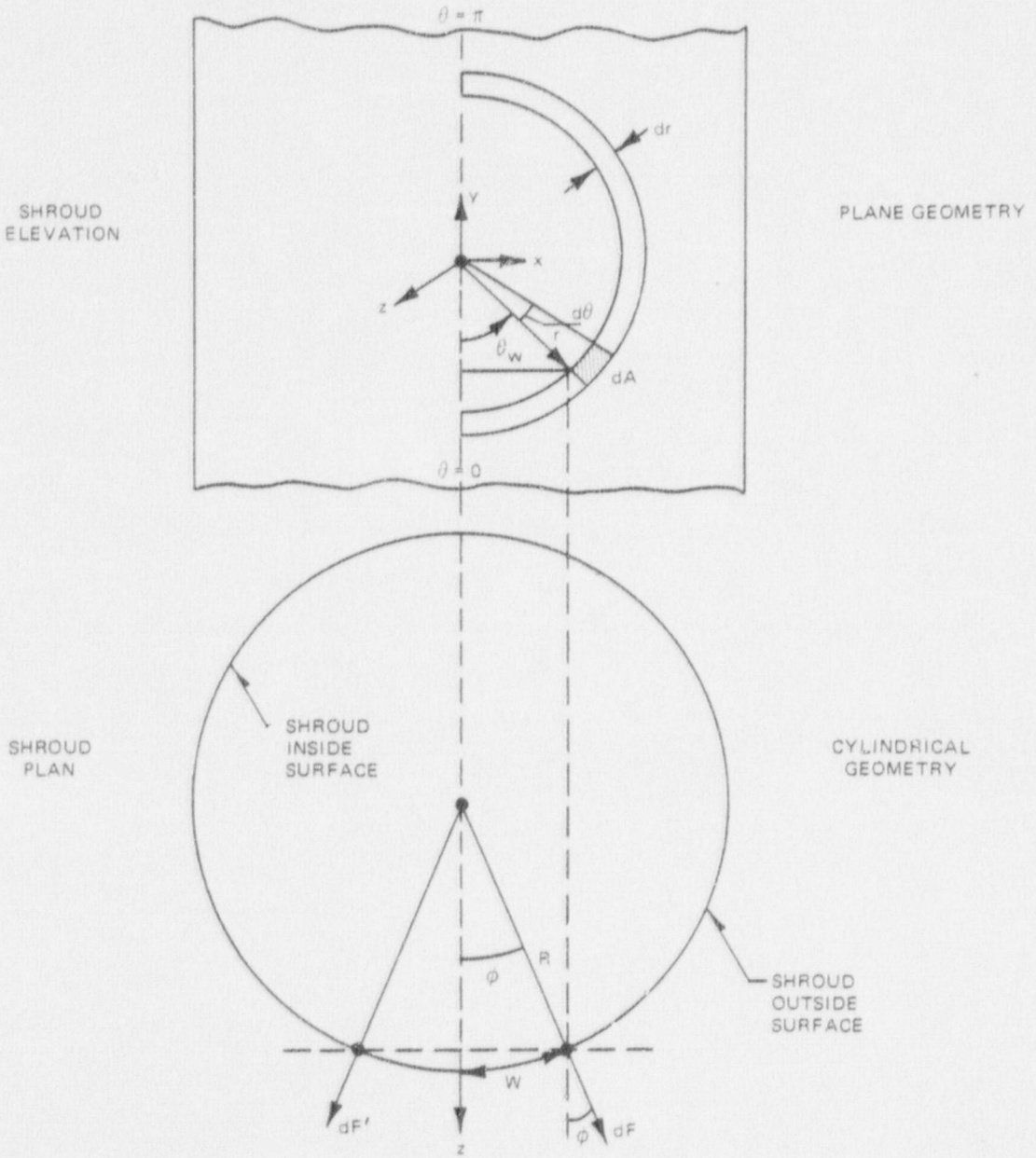

Figure 3-1. Calculation of Total Shroud Load

The total outward force on the shroud F is obtained by integration, and is directed outward along the recirculation suction nozzle centerline:

$$F_s = 2 \int_{r=0}^{r_{max}} \Delta P(r) r dr \int_{0}^{\pi} \cos\left(\frac{r \sin\theta}{R}\right) d\theta$$

A discrete integration is done on both r and θ, since r varies discretely from junction to junction, as shown on Figure 2-9. The equivalent summation is

$$F_s = 2 \sum_{i=0}^{N} \Delta P_i r_i \Delta r \cdot \frac{\pi}{180} \sum_{j=1}^{180} \cos\left(\frac{r_i \sin j}{R}\right)$$

where

- i = radius index
- N = maximum number of radii considered
- r_i = radius of ith junction as follows:
  - r_0 = centerline radius = 0
  - r_1 = junction (8) radius = Δr
  - r_2 = junction (12) radius = $2\Delta r$
  - .
  - .
  - .
  - r_N = last junction radius = $N\Delta r$
- Δr = junction spacing (constant, see Figure 2-9)
- ΔP_i = pressure differential at ith junction
- j = degree index
- R = shroud outer surface radius
- F_s = total force pushing shroud outward at a given instant in time.

To simplify the integration, only positive ΔP_i are considered; if constructive wave interference causes ΔP_i to be negative, the ΔP_i in the summation is set to zero.

Note that there are only 12 junctions on the shroud surface (junctions (8), (12), (17), (22), (27), (32), (37), (42), (47), (52), (57), and (62)) where WHAM pressures are used. (Junction (67) is not used because of its proximity to the edge of the network.) It is seen from Figure 2-10 that for times beyond 2.22 msec the wave begins to extend radially beyond the end of the WHAM network. Since all available network dimensions are being used in WHAM, another method is needed to extrapolate the wave beyond the WHAM network for purposes of calculating the shroud loading. The method presently used adds additional fictitious junction points along the shroud surface. Enough fictitious junction points are added beyond junction (62) such that the junction pressure approaches 1000 psi at 5 psi per junction, starting with the junction (62) pressure, and continuing until the junction pressure is within 5 psi of 1000 psi. Examples best illustrate this linear extrapolation procedure:

- At a given time, suppose the junction (62) pressure is 997 psi. Then, since the junction (62) pressure is within 5 psi of 1000 psi, no fictitious junctions are added.

- Suppose the junction (62) pressure is 987 psi. Then fictitious node 67 with pressure 992 psi is added, and fictitious node 72 with pressure 997 psi is added, before the force summation is performed.

The value of N, the maximum number of radii considered, is the total number of real and fictitious junction points.

The area on the shroud surface which is experiencing real and fictitious pressure differentials is also computed. The total force or load on the shroud and the area of application of the force are shown on Figures 3-2, 3-3, and 3-4 for the three BWR/6 sizes. Note that the area of application decreases after reaching its peak value; because, when the differential pressure of a particular radius is less than 5 psi or negative, the area of that radius does not contribute to the area of application.

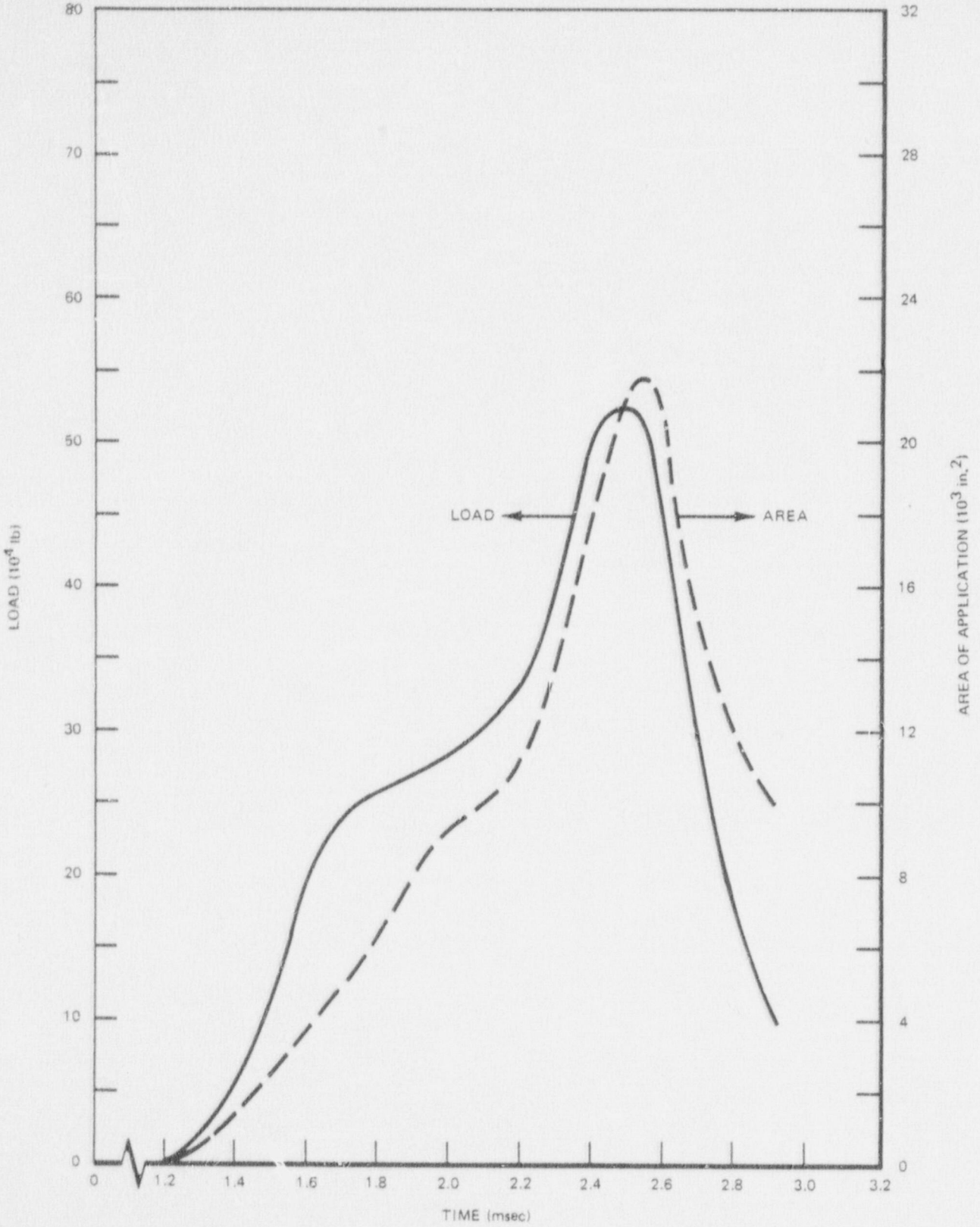

Figure 3-2. Acoustic Load on Shroud of BWR/6-218

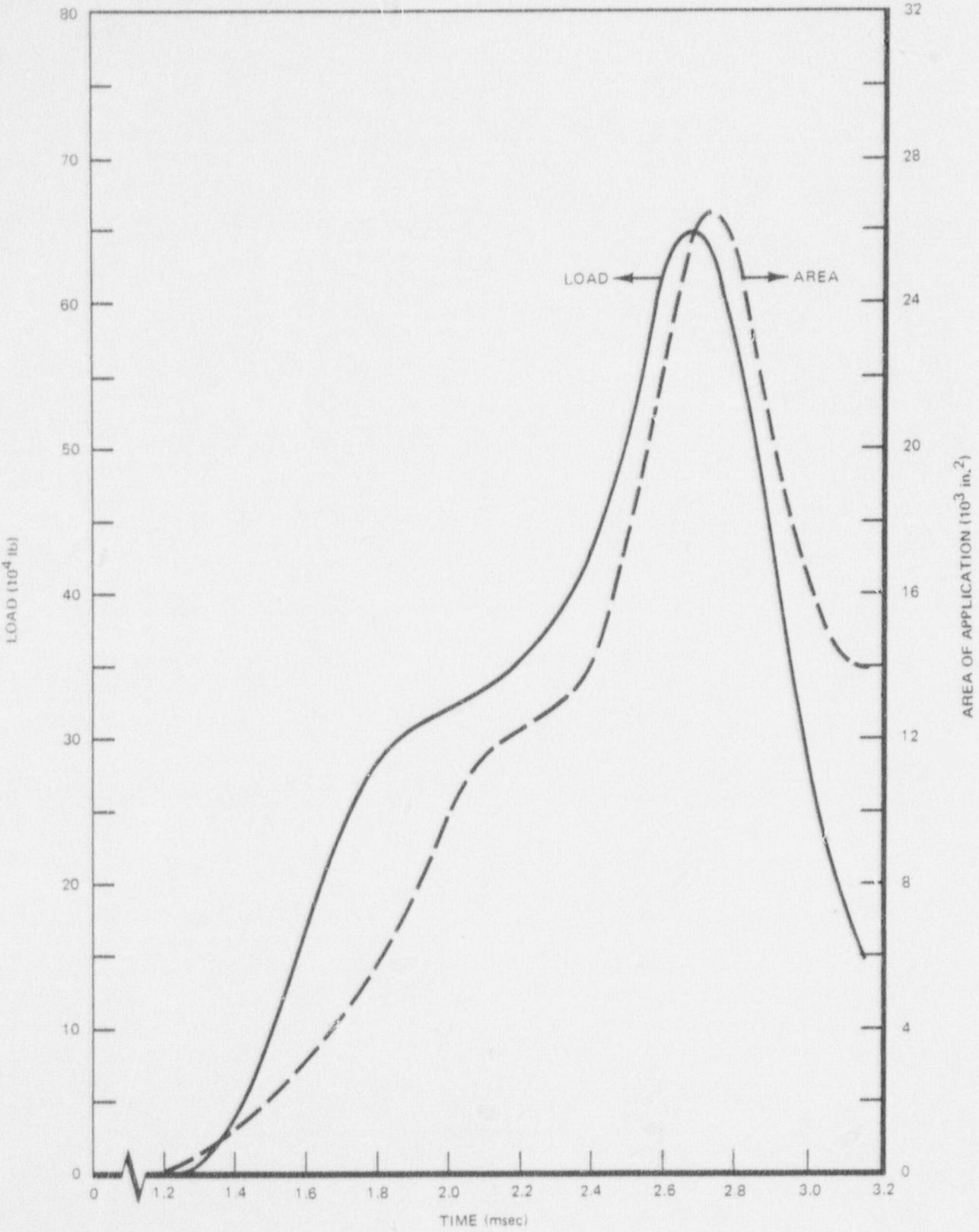

Figure 3-3. Acoustic Load on Shroud of BWR/6-238

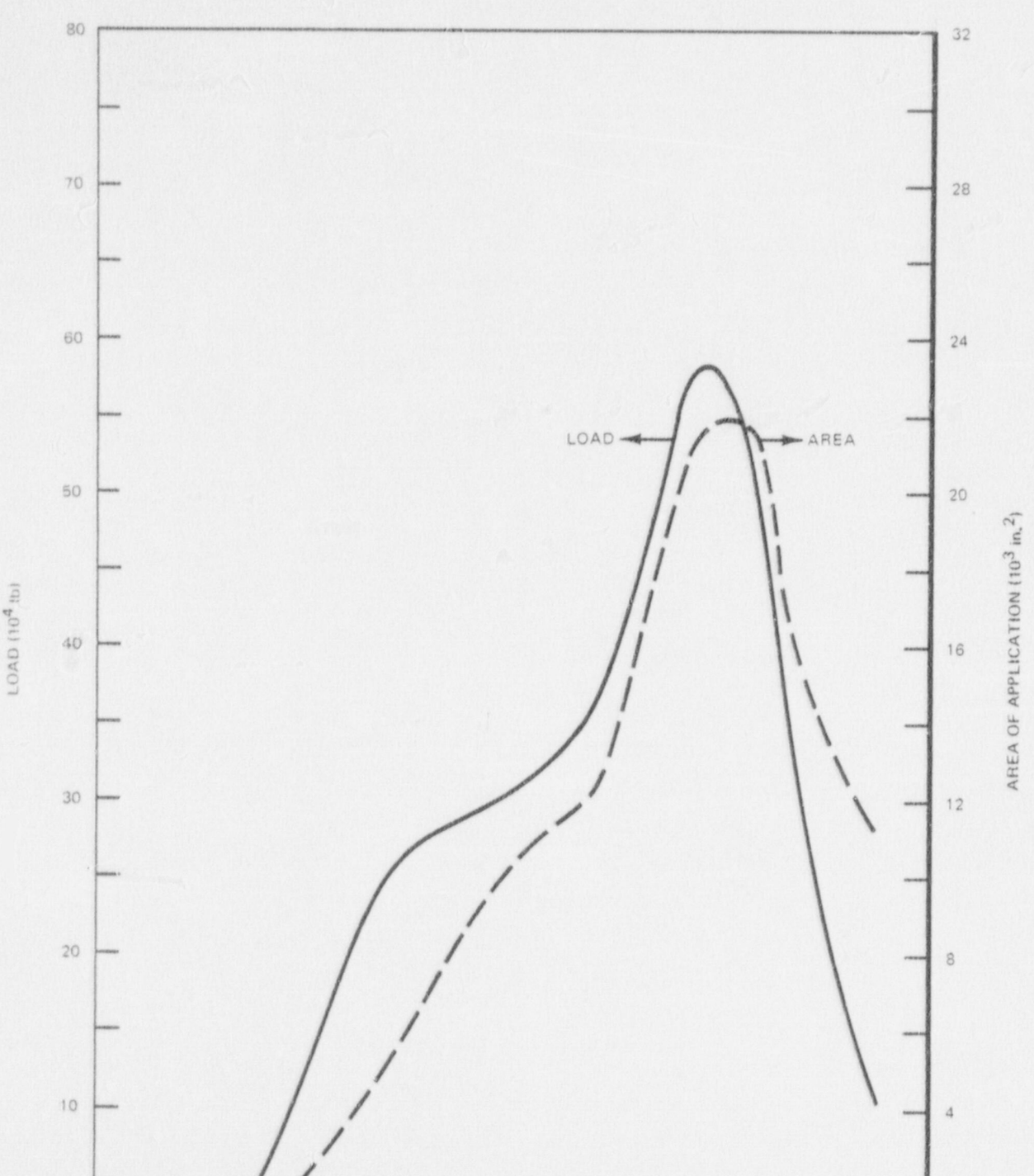

Figure 3-4. Acoustic Load on Shroud of BWR/6-251

3.2 STRUCTURAL RESPONSE OF THE SHROUD

The dynamic response of the shroud (BWR/6-238) for the acoustic loads described above is computed using a finite shell model compatible with the ASHSD computer program.[8] The structure is treated as being axisymmetric and the time-dependent loading is considered to be arbitrary or asymmetric. The load at each elevation and for each time interval is decomposed using Fourier series expansion around the circumferential direction. The finite element model (Figure 3-5) of the structure includes the shroud support legs, shroud support plate, shroud, core plate, top guide, shroud head and steam separator assembly, and the inertial effects of the fuel bundles and guide tubes. In addition, mass effects of the contained water is also included by lumping the water mass at appropriate nodal points.

The first 15 harmonic components of the loading are considered in the time history analysis using the direct integration method. A form of viscous damping, proportional to the mass and stiffness matrices, is considered in the analysis.

From the results of the analysis, the maximum moments and forces in the hoop and meridional directions during the entire time history are determined. These are used to compute maximum membrane and bending stresses in the shroud. The calculated stress due to acoustic loading of 19,100 psi is well within the value used in the shroud stress report for acoustic loading which was based on an equivalent static load. The calculated design stresses as reported in the shroud stress report are all within the ASME Code-allowable stresses.

Based on this analysis, it is also concluded that the designs of BWR/6-218 and BWR/6-251 shrouds are adequate for the acoustic loads due to a recirculation line break.

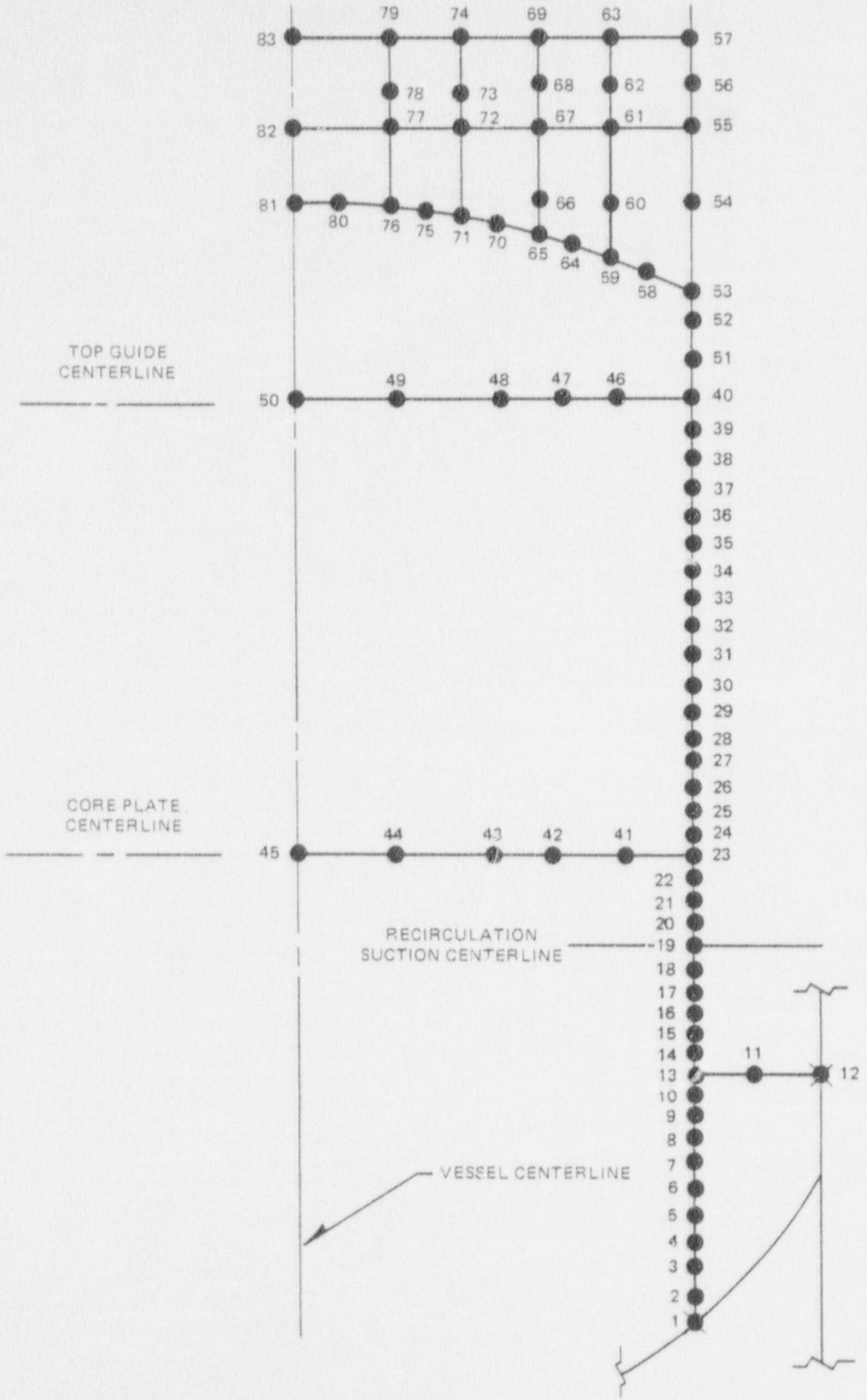

Figure 3-5. Finite Element Model for the Shroud

4. SHROUD SUPPORT PLATE LOAD AND STRUCTURAL RESPONSE

4.1 SHROUD SUPPORT PLATE LOAD

Calculation of the acoustic load on the shroud support plate (see Figure 1-1) is also done by a separate calculation. The radial pressure distribution provided by WHAM is used in the manner shown on Figure 4-1 to compute the differential pressure distribution across the shroud support.

The shroud support plate is modeled as a straight strip, whose width is the distance between the vessel inner wall and the shroud outer surface. Starting from a point directly beneath the recirculation suction nozzle, one half of the strip is divided into areas A, B, C ... depending on where the radii of the WHAM junctions intersect the strip. At a particular time, the pressure associated with each area is the acoustic pressure of each associated WHAM junction, as shown on Figure 4-1. Area "A" is a special case whose pressure is determined by linear interpolation between two junction pressures. In the example of Figure 4-1, the shroud support plate distance from the recirculation suction nozzle centerline is such that the shroud support plate lies between junctions (37) and (42). The values of the dimension "H" on Figure 4-1 are given in Table 4-1.

The number of shroud support plate areas A, B, C ... is determined by the number of real plus fictitious junctions. The pressure differential acting on each area is

$$\Delta P_i = 1000 - P_i \text{ psi}$$

where

P_i = junction pressure associated with the area, psi
1000 = assumed pressure below shroud support plate, psi

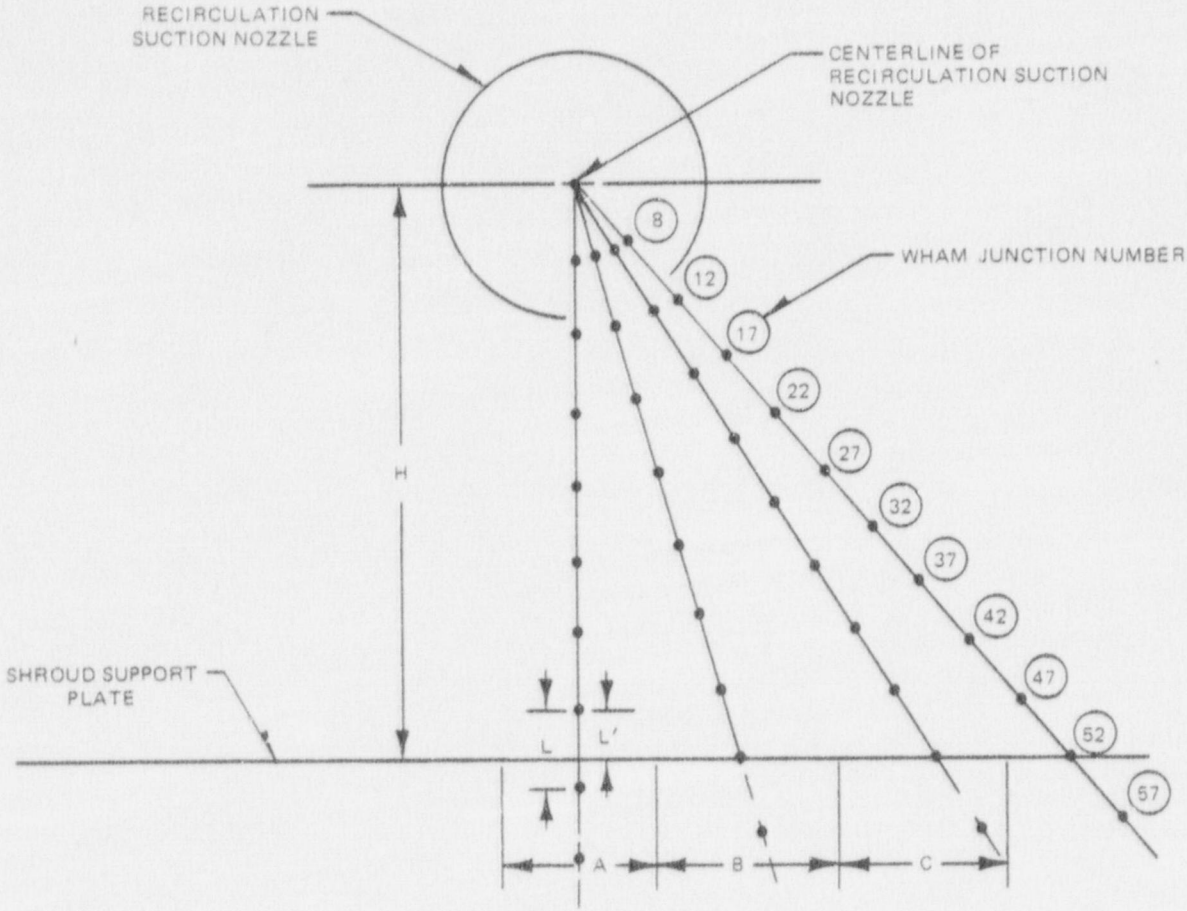

PRESSURE ON AREA "A" = $P_{37} + (P_{42} - P_{37}) \left(\frac{L'}{L}\right)$

PRESSURE ON AREA "B" = P_{42}

PRESSURE ON AREA "C" = P_{47}

Figure 4-1. Calculation of Shroud Support Plate Load

Table 4-1

DISTANCE FROM SHROUD SUPPORT PLATE TO
RECIRCULATION SUCTION NOZZLE CENTERLINE

BWR/6 Vessel i.d. (in.)	Distance (in.) (dimension H)
218	33.0
238	27.5
251	32.0

The total loading acting at a particular instant of time is

$$F_{ss} = 2\left\{\Delta P_A A_A + 2[\Delta P_B A_B + \Delta P_C A_C + \ldots]\right\}$$

where

ΔP_A = pressure differential on area A

A_A = square inches in area A

$2[\ldots]$ = factor of 2 to account for pairs of areas B, C, D ... etc.

$2\{\ \}$ = factor of 2 to account for doubling of pressure differential when acoustic wave is reflected upward from shroud support plate

F_{ss} = total force on shroud support plate acting upwards at a point on the shroud support directly under the recirculation suction nozzle centerline.

The latter factor of 2 is needed because WHAM does not explicitly model the pressure of the shroud support plate in the EPN of Figure 2-9. If WHAM did account for the presence of the shroud support, it would predict a doubling of the wave pressure differential as the wave reflected upward off the rigid surface.

The shroud support loadings for the three sizes of BWR/6 are shown on Figures 4-2, 4-3, and 4-4. The area of application is also shown on these figures. The area of application is subject to the same rule which is used to determine the area

of application of the shroud loading; namely, if the differential pressure of a given area is less than 5 psi or negative, then that area does not contribute to the area of application.

4.2 STRUCTURAL RESPONSE OF THE SHROUD SUPPORT PLATE

The peak loads from Figure 4-2, 4-3, and 4-4 are expressed as a differential pressure on the shroud support plate and directly added to the differential pressure during normal operation. This pressure sum is found to be less than the maximum faulted category differential pressure values during the subsequent blowdown. In addition, the overturning moments on the shroud due to the shroud plate vertical localized acoustic pressure differences is found to be very small when compared to the design load.

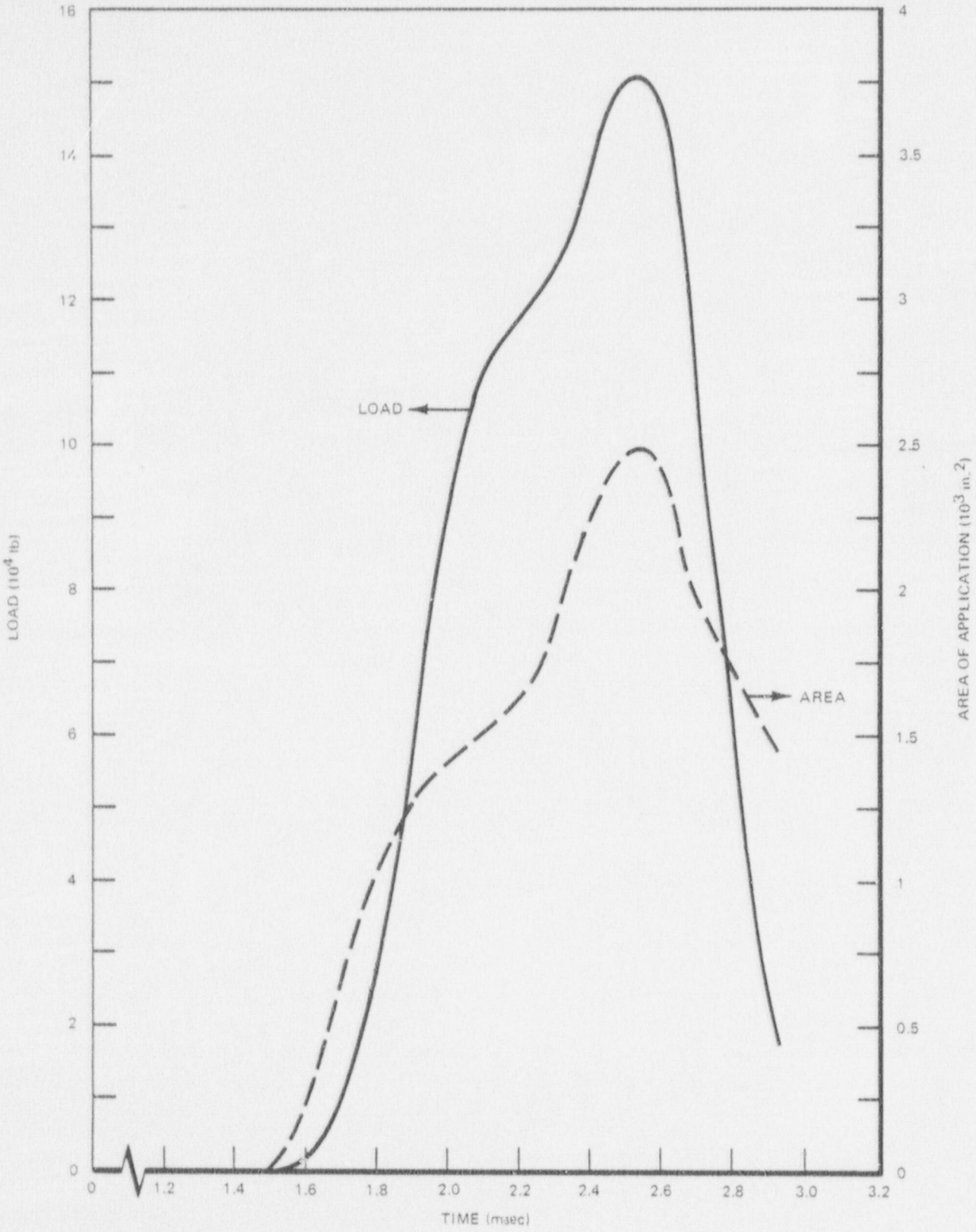

Figure 4-2. Acoustic Load on Shroud Support Plate of BWR/6-218

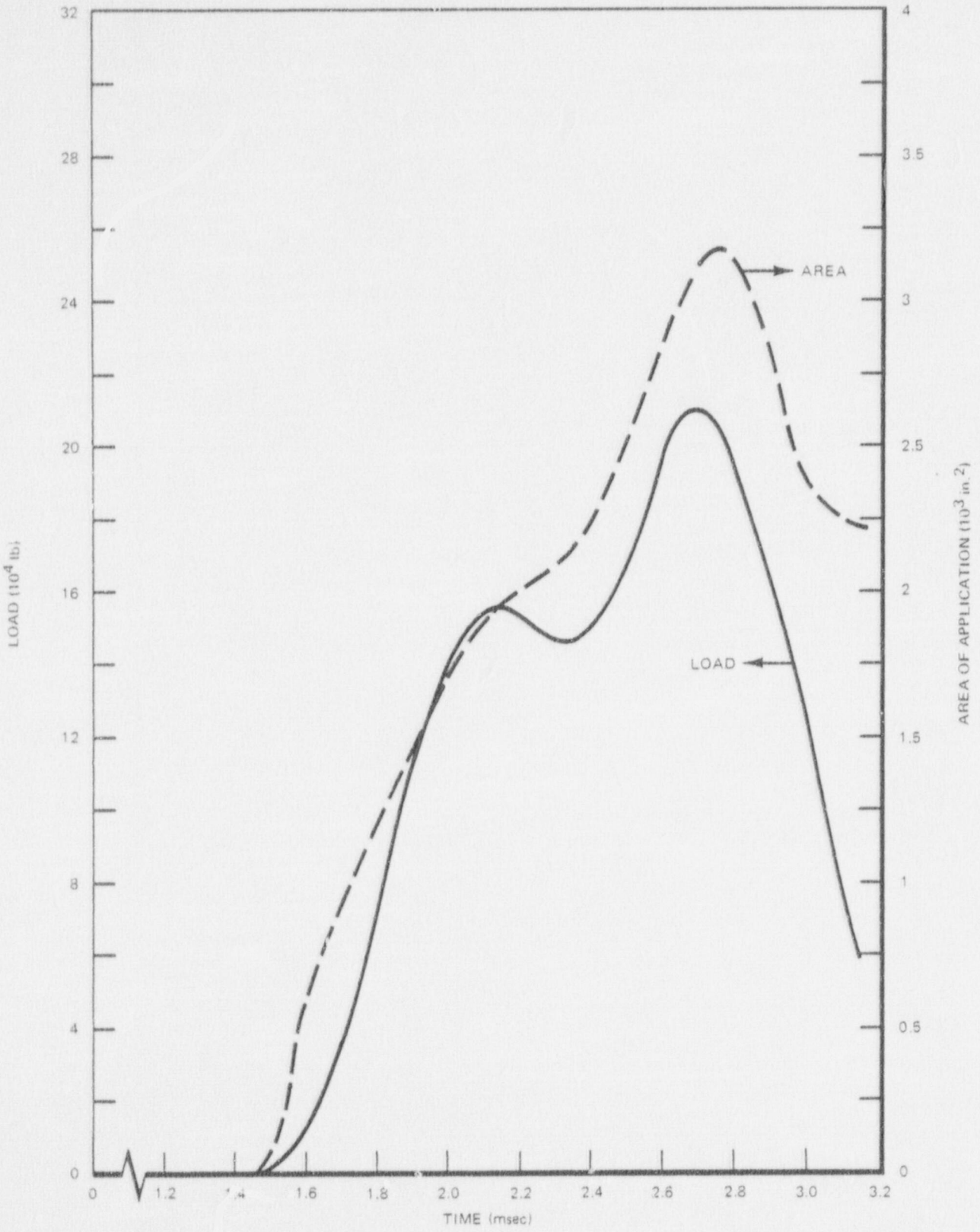

Figure 4-3. Acoustic Load on Shroud Support Plate of BWR/6-238

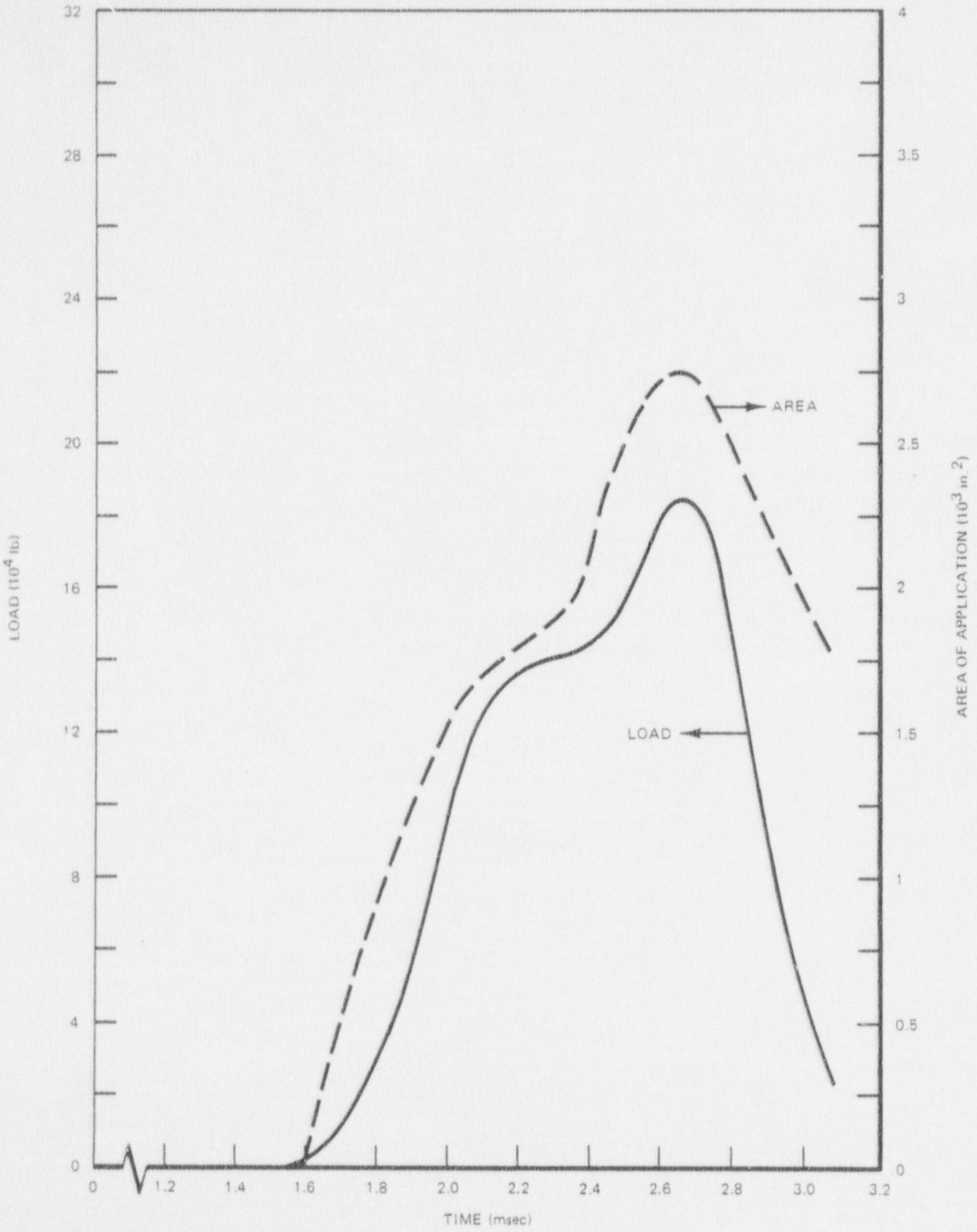

Figure 4-4. Acoustic Load on Shroud Support Plate of BWR/6-251

5. JET PUMP LATERAL LOAD AND STRUCTURAL RESPONSE

5.1 JET PUMP LATERAL LOAD

The calculation of the lateral load imposed by the passage of the initial acoustic wave on the jet pump nearest to the recirculation suction nozzle is done separately from WHAM. The radial pressure distribution from WHAM is used to calculate the instantaneous acoustic pressures along the near side and far side of the jet pump, as shown in (a) of Figure 5-1.

The total forces acting individually on the near and far sides of the jet pump are calculated similarly to the total force on the shroud support plate. It is assumed that initially the pressure on the near and far sides are both equal to 1000 psi. The values of X_N and X_F, the distances from the centerline of the recirculation suction nozzle to the near and far sides, respectively, of the jet pump are used in the same way the dimension "H" was used in the calculation of the shroud support plate loads (see Figure 4-1). Values of X_N and X_F are tabulated for the two larger sizes of BWR/6 in Table 5-1.

Pressure differentials on the jet pump below the shroud support plate or above the top of the jet pump are not calculated in the cases where the extrapolation procedure would cause the total of the real and fictitious junction points to extend beyond the bottom or the top of the jet pump.

The WHAM code does not explicitly model the presence of the jet pumps in the EPN of Figure 2-9. Therefore, a method has been developed to apply appropriate wave reflection factors to the differential pressure distribution computed for the near side of the jet pump. The jet pump is divided into a number of vertical sections, where each section has a characteristic outer diameter associated with it, as shown for a typical section "i" in (b) of Figure 5-1. The near side wave reflection factor for section "i" is given by

$$R_i = \frac{2}{1 + \frac{D - d_i}{D}}$$

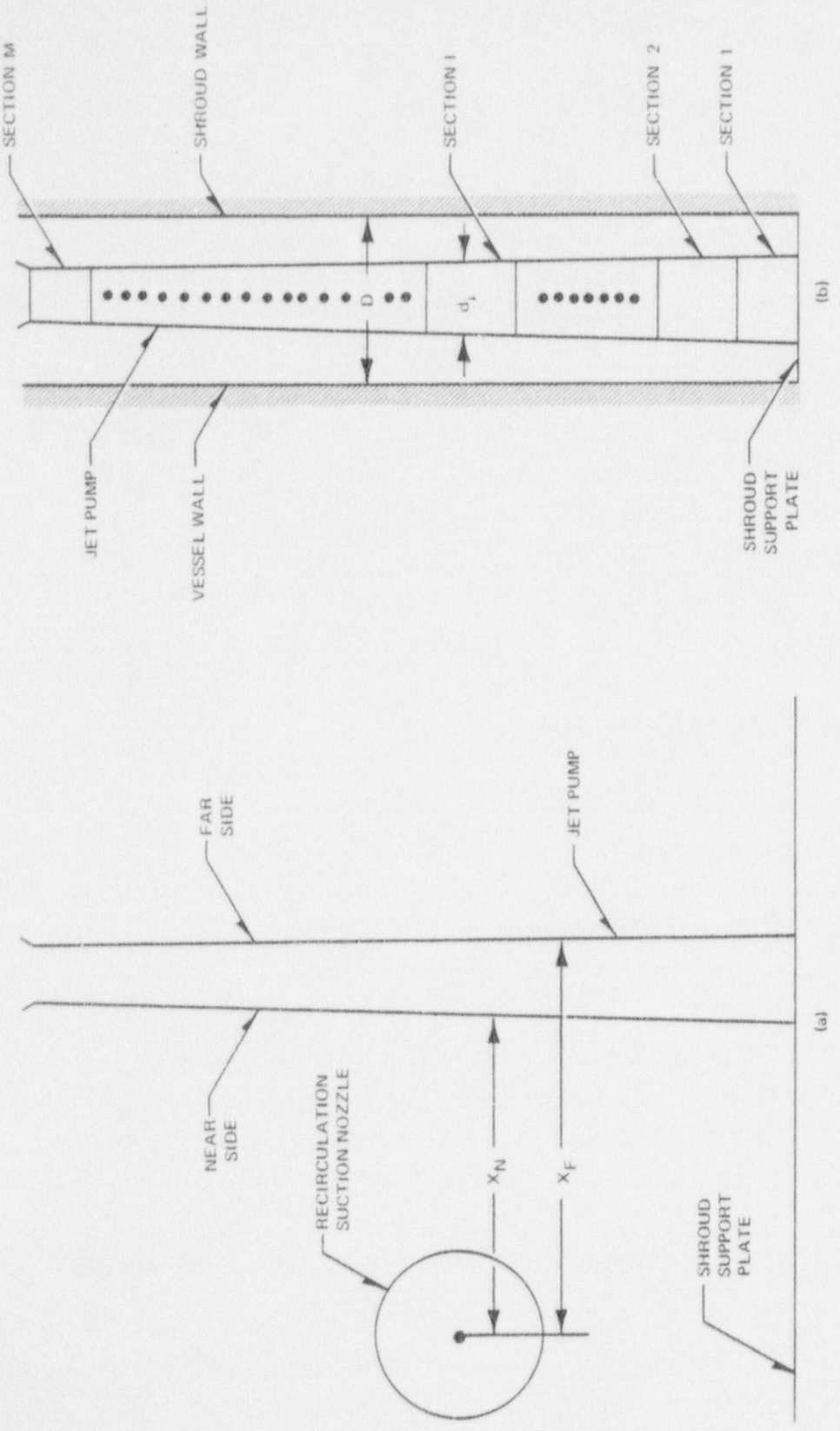

Figure 5-1. Calculation of Jet Pump Lateral Load

Table 5-1

DISTANCE TO NEAR AND FAR SIDES OF JET PUMP
FROM RECIRCULATION SUCTION NOZZLE CENTERLINE

BWR/6 Vessel i.d. (in.)	Near Side Distance X_N (in.)	Far Side Distance X_F (in.)
238	36	50
251	32	45

where D = constant distance between the vessel inner wall and the outer shroud surface (see Table 2-1)

d_i = outer diameter of vertical section i
R_i = reflection factor for section i

The reflection factor is 1 when d_i is zero, and is 2 when d_i is equal to D. This means that if the jet pump were not present ($d_i = 0$) then there would be no increase in the pressure wave ($R_i = 1$); and if the jet pump filled the gap between vessel and shroud completely, the pressure wave would double ($R_i = 2$).

The net load on the vertical section "i" is then the difference between the near side force with the reflection factor applied and the far side force:

$$F_{net,i} = A_i [R_i \Delta P_{N,i} - \Delta P_{F,i}]$$

where

A_i = cross-sectional area of section i
$\Delta P_{N,i}$ = near side pressure differential of section i, 1000 - $P_{N,i}$
$\Delta P_{F,i}$ = far side pressure differential of section i, 1000 - $P_{F,i}$

It is seen that applying no reflection factor to the far side pressure differential maximizes the net lateral force on section i, $F_{net,1}$.

The total lateral load on the jet pump at a given instant is the sum of the net lateral forces on all the vertical cross sections:

$$F_{LJP} = \sum_{i=1}^{M} F_{net,i}$$

The total lateral load on the jet pump F_{LJP} is in the direction of the recirculation suction nozzle.

The total cross-sectional jet pump area over which the acoustic load is applied is also calculated. Figures 5-2 and 5-3 show the total lateral load and the area of application for the two larger sizes of BWR/6.

5.2 STRUCTURAL RESPONSE OF THE JET PUMP

The jet pump for BWR/6-238 is evaluated for the described acoustic loads by performing a dynamic analysis. The jet pump along with riser and brace, tie-beam, inlet-mixer, and diffuser are modelled using three-dimensional beam elements and pipe elements with fixity at the diffuser base (see Figures 5-4 and 5-5). Nodal masses include metal and hydrodynamic masses from both inside and outside of the jet pump. The acoustic load shown in Figure 5-2 is distributed to the nodes based on the tributary area to each node, and a dynamic analysis using a time-history mode superposition method is performed.

The results of the analysis are evaluated to determine the maximum shear and bending moments. These occur at the diffuser base with a maximum bending stress of 4800 psi and a maximum shear stress of 1000 psi. These stresses are very small. Further, the maximum bending stress is well within the values computed in the design of the jet pump, using a simplified analysis.

Based on this analysis, it is concluded that the designs of the BWR/6-218 and BWR/6-251 jet pumps are also adequate for the acoustic loads due to a recirculation break.

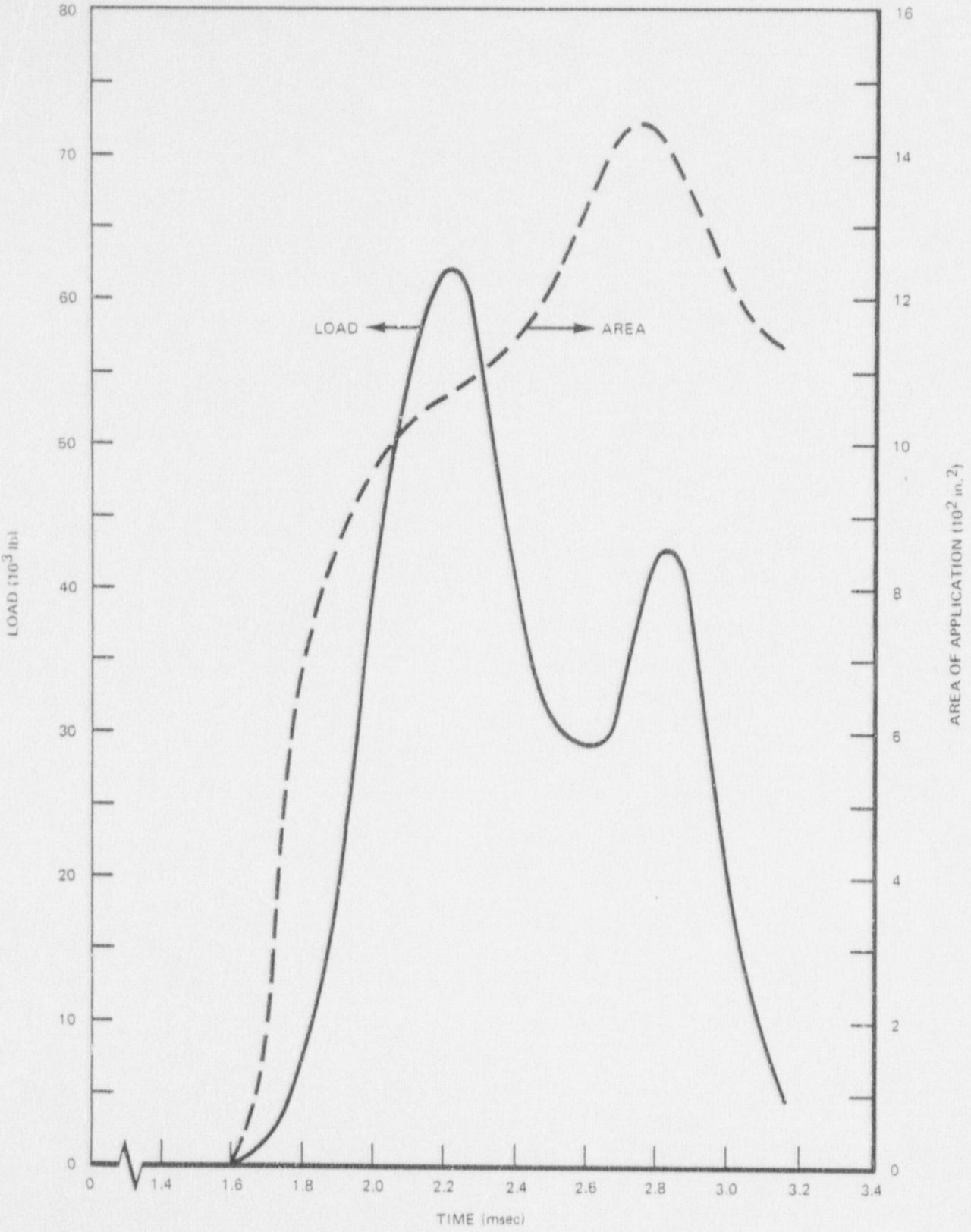

Figure 5-2. Lateral Acoustic Load on Jet Pump of BWR/6-238

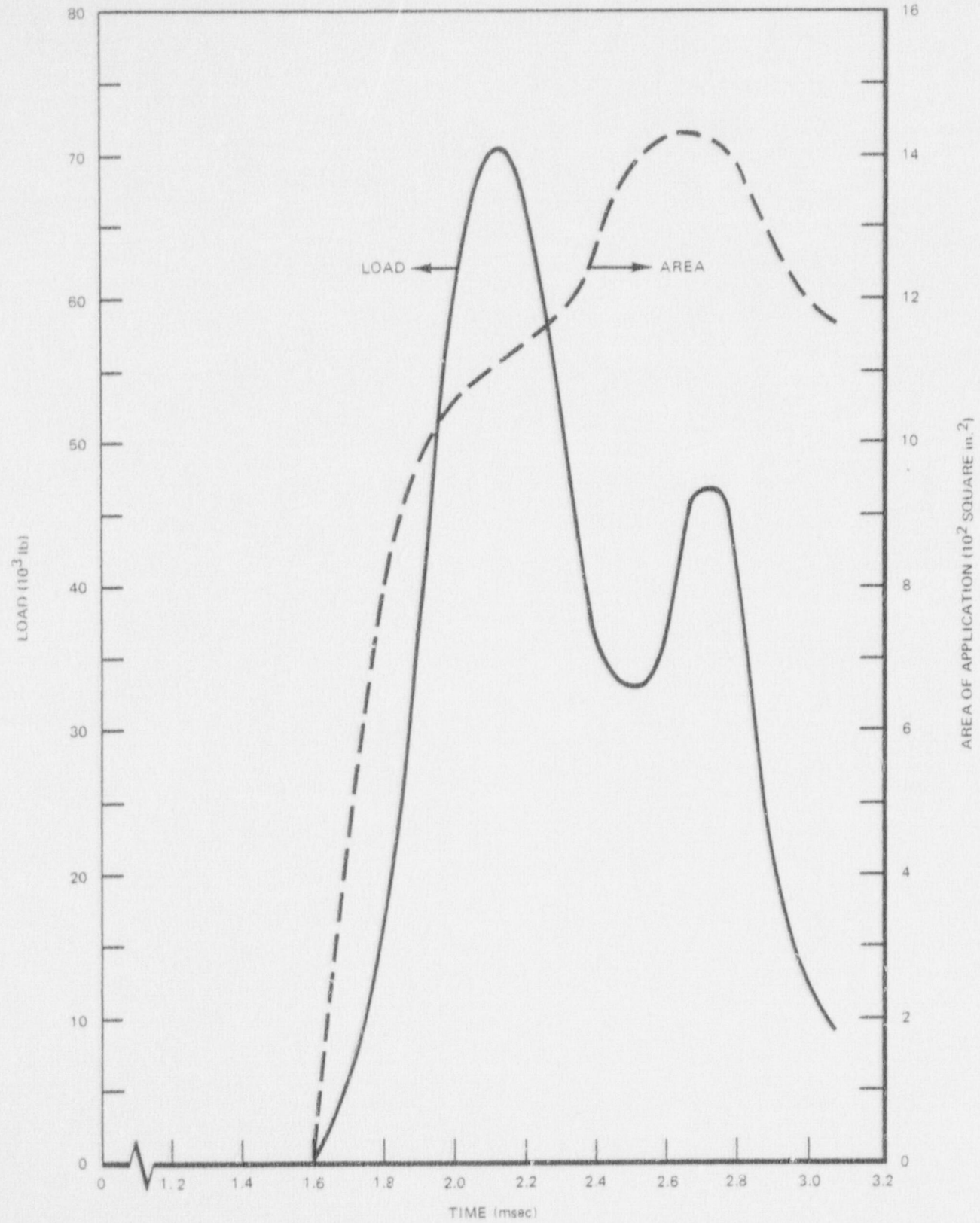

Figure 5-3. Lateral Acoustic Load on Jet Pump of BWR/6-251

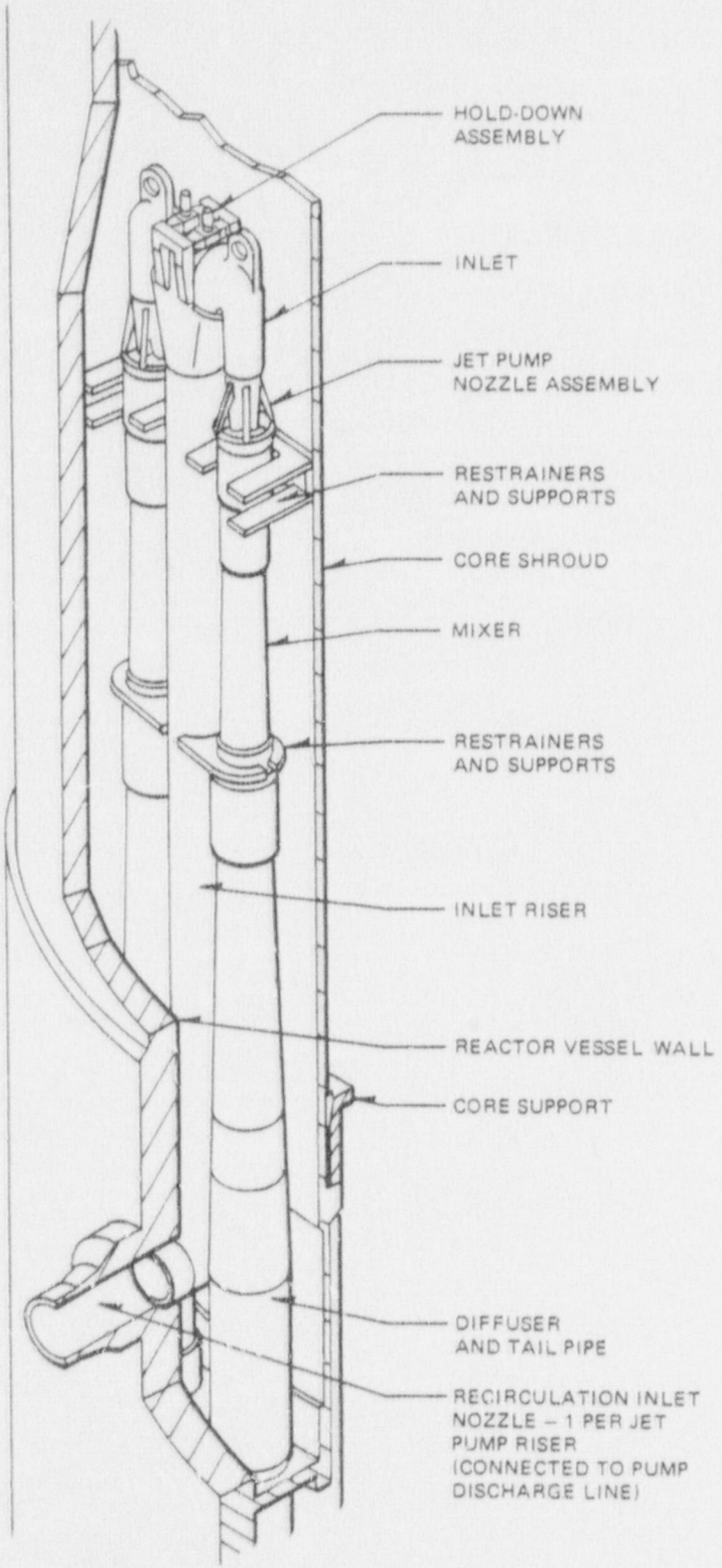

Figure 5-4. BWR/6 Jet Pump Assembly

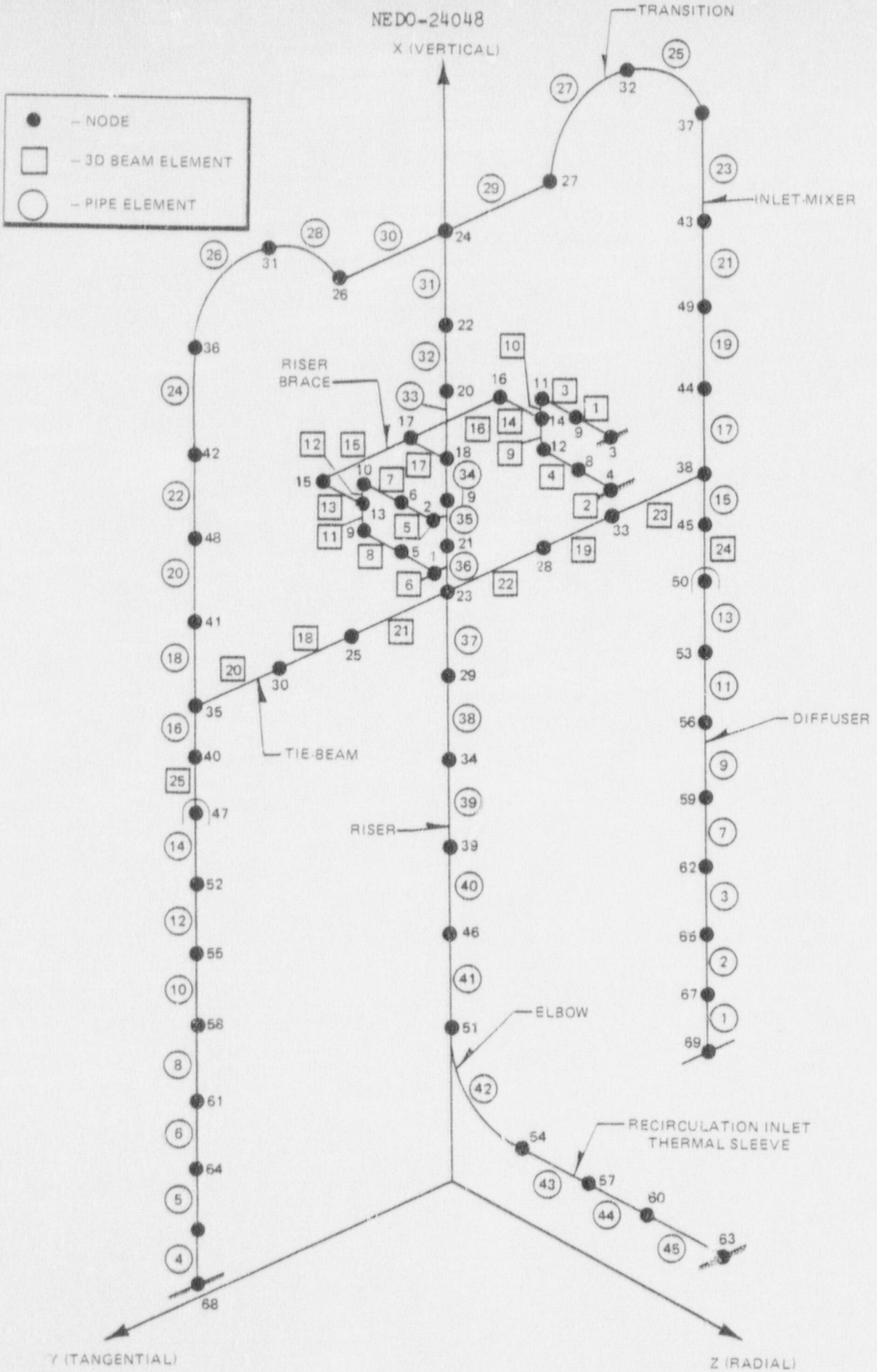

Figure 5-5. Finite Element Model for the Jet Pump

6. LOAD SUMMARY

Table 6-1 summarizes the description and magnitude of the acoustic loads treated in this report.

Table 6-1

ACOUSTIC LOADS SUMMARY

Description of Loads	Magnitude of Loads BWR/6 218	BWR/6 238	BWR/6 251
Shroud (loads act toward broken recirculation line)			
Maximum load applied over projected recirculation line area.	148 psi	146 psi	150 psi
Maximum average pressure (total load/area of application).	55 psi	55 psi	55 psi
Maximum integrated lateral load.	525,000 lb	645,000 lb	580,000 lb
Shroud Support Plate (loads act vertically upward)			
Maximum average pressure (total load/area of application).	78 psi	83 psi	75 psi
Maximum integrated vertical load.	152,000 lb	212,000 lb	190,000 lb
Jet Pump Risers and Diffusers			
Lateral loads on jet pump diffusers and mixing selections of the jet pumps closest to the postulated recirculation line break.			
Maximum average lateral pressure in direction of broken line.	58 psi*	59 psi	63 psi
Maximum integrated lateral load in direction of broken line.	62,300 lb*	62,300 lb	71,000 lb

*Estimated from BWR/6-238 and BWR/6-251 loads

7. REFERENCES

1. A. R. Edwards and T. P. O'Brien, "Studies of Phenomena Connected with the Depressurization of Water Reactors," Journal of British Nuclear Energy Society, 9, (2), April 1970.

2. B. O. Borgartz et al., "Depressurization Studies for Water Reactors - Measurement of Transient Two Phase Density, Pressure and Temperature Changes Following the Sudden Depressurization of a 206mm Internal Diameter (8 inch Nominal Bore) Pipe (Test 1)," AWRE/44/86/97, SRD R29, June 1974.

3. B. O. Borgartz et al, "Decompression Studies - Phase 3: Results of Tests 142 and 143," AWRE/44/86/141, SRD R76, August 1977.

4. G. E. Gruen, "WHAM Prediction of Semiscale Test Results," Idaho Nuclear Corporation report IN-1431, October 1970.

5. G. L. Sozzi and N. A. Fedrick, *Decompression Waves in a Pipe and Vessel Containing Subcooled Water at 1000 Psi*, March 1973 (NEDE-13333), approved for release, December 1977.

6. S. Fabic, "Computer Program WHAM for Calculation of Pressure, Velocity, and Force Transients in Liquid Filled Piping Networks," Kaiser Engineers Report No. 67-49-R, November 1967.

7. S. Fabic, "Two and Three-Dimensional Fluid Transients," Westinghouse Electric Corporation, Paper submitted for presentation at the 17th annual meeting of the American Nuclear Society, Boston, Massachusetts, June 13-17, 1971, Log No. B 385.

8. S. Ghosh and E. Wilson, "Dynamic Stress Analysis of Axisymmetric Structures Under Arbitrary Loading," Report No. EERC-10, U.C. Berkeley, California, 1969 (Revised in September 1975).

NUCLEAR ENERGY DIVISIONS • GENERAL ELECTRIC COMPANY
SAN JOSE, CALIFORNIA 95125

GENERAL ELECTRIC

TECHNICAL INFORMATION EXCHANGE

TITLE PAGE

AUTHOR	SUBJECT	TIE NUMBER 77NED172
T. W. Craig	Nuclear Science and Technology	DATE September 1978
TITLE Evaluation of Acoustic Pressure Loads on BWR/6 Internal Components		GE CLASS I GOVERNMENT CLASS
REPRODUCIBLE COPY FILED AT TECHNICAL SUPPORT SERVICES, R&UO, SAN JOSE, CALIFORNIA 95125 (Mail Code 211)		NUMBER OF PAGES

SUMMARY

Acoustic loads act on reactor vessel internals immediately after a postulated severance of a recirculation suction line at the reactor vessel nozzle. These loads result from pressure differentials across the internals, which are caused by decompression waves traveling at the speed of sound through subcooled water. The internal structures subject to acoustic loads are the shroud, shroud support plate, and jet pumps.

To assess the design adequacy of these internal structures to acoustic loads, the behavior of the acoustic waves must be known. General Electric uses the WHAM code to predict acoustic wave transients. The application of WHAM to BWR/6 is described, and the acoustic loads are defined. Structural evaluations for these loads are briefly discussed.

It is concluded that the acoustic loads are calculated in a conservative manner for the affected vessel internals. Further, the internals are adequate to resist these loads.

By cutting out this rectangle and folding in half, the above information can be fitted into a standard card file.

DOCUMENT NUMBER NEDO-24048

INFORMATION PREPARED FOR NED

SECTION BWRPD

BUILDING AND ROOM NUMBER 1900 930 MAIL CODE 194

GENERAL ELECTRIC